

CRBRP-3

**HYPOTHETICAL CORE DISRUPTIVE
ACCIDENT CONSIDERATIONS IN CRBRP**

VOLUME 2:

**ASSESSMENT OF THERMAL MARGIN BEYOND
THE DESIGN BASE**

CLINCH RIVER BREEDER REACTOR PLANT

8208060167 820804
PDR ADOCK 05000537
A PDR

CHANGE CONTROL RECORD		TITLE	DOCUMENT NO.
		Hypothetical Core Disruptive Accident Considerations in CRBRP Volume 2 Assessment of Thermal Margin Beyond the Design Base	CRBRP-3 Volume 2
REV NO./DATE	CHANGE RELEASE DOCUMENT	PAGES AFFECTED	REMARKS
0/March 80		All	First formal issue of document
Rev 1/5-81		i, 2-4, 2-6, 2-7, 2-10 thru 2-16, 2-24, 2-25, 2-26, 2-32, 2-34, 2-43, 2-44, 2-76	Pages added 2-16A thru 2-16G, 2-34A
Rev 2/10-81		2-16B, 2-16C, 2-16F, 2-16G	
Rev 3/2-82		i, 2-4, 2-18	Page added 2-18A
Rev 4/6-82		ii, iii, vii, xi, xiii, xxiii, 2-7, 2-8, 2-10, 2-76, 2-78, 3-24, 4-10, 4-19, 4-24, A-1 to A-25, C.1-3, C.1-12, C.1-18, C.3-19, G.2-1, G.2-3, G.4-4 to G.4-6, H.0-1, H.1-4, H.1-5, H.1-9, H.3-1 to H.3-7	Pages added 2-10A, 2-10B Revised Appendix A Added Section H.3

TABLE OF CONTENTS

	<u>Page</u>
1.0 INTRODUCTION	1-1
1.1 REFERENCES	1-5
2.0 DESIGN FEATURES PROVIDING THERMAL MARGIN BEYOND THE DESIGN BASE	2-1
2.1 TMBDB FEATURES REQUIREMENTS	2-2
2.1.1 General	2-2
2.1.2 Feature Requirements	2-3
2.1.3 Maintenance and Testing Requirements for TMBDB Features	2-16A 1
2.2 DESCRIPTION OF DESIGN FEATURES	2-17
2.2.1 Reactor Cavity to Containment Barrier	2-17
2.2.2 Reactor Cavity Penetrations and Recirculating Gas Cooling System	2-18 3
2.2.3 Guard Vessel Support	2-18
2.2.4 Reactor Cavity and Pipeway Cell Liners	2-18A 3
2.2.5 Reactor Cavity and Pipeway Cell Liner Vent System	2-19
2.2.6 Reactor Cavity Vent System	2-22
2.2.7 Containment Purge Capability	2-24
2.2.8 Containment Vent Capability	2-25
2.2.9 Containment Cleanup System	2-26
2.2.10 Annulus Air Cooling System	2-27
2.2.11 Containment System Leakage Barrier	2-29
2.2.12 TMBDB Instrumentation System	2-30
2.2.13 Electrical Power System	2-34
2.2.14 Containment Structures	2-34
2.2.15 Control Room Habitability	2-35
2.3 OPERATOR ACTION SEQUENCE	2-38
2.4 REFERENCES	2-41
3.0 ASSESSMENT OF THERMAL MARGIN	3-1
3.1 THERMAL MARGIN WITHIN THE REACTOR VESSEL	3-2
3.1.1 Core Debris Distribution	3-2
3.1.2 In-Vessel Debris Retention Capability	3-10
3.1.3 Secondary Criticality Considerations	3-15
3.1.4 Penetration of the Reactor and Guard Vessels	3-15
3.2 THERMAL MARGIN EXTERNAL TO THE REACTOR VESSEL	3-18
3.2.1 Scenario	3-18
3.2.2 Containment Transients Prior to Sodium Boildry	3-26
3.2.3 Containment Transients After Sodium Boildry	3-60
3.2.4 Secondary Criticality Considerations (Ex-Vessel)	3-70

TABLE OF CONTENTS (Continued)

	<u>Page</u>
3.3 CONCLUSIONS ON THERMAL MARGIN BEYOND THE DESIGN BASE	3-72
3.4 REFERENCES	3-73
4.0 ASSESSMENT OF RADIOLOGICAL CONSEQUENCES	4-1
4.1 HCDA RADIOLOGICAL SOURCE TERM	4-1
4.1.1 Non-Energetic Core Meltdown	4-2
4.1.2 Energetic HCDA	4-5
4.2 RADIOLOGICAL DOSES FROM ATMOSPHERIC RELEASES	4-8
4.2.1 Methods and Data Base	4-8
4.2.2 Radiological Doses	4-10
4.3 GROUNDWATER CONSIDERATIONS	4-11
4.4 HETEROGENEOUS CORE CONSIDERATIONS	4-13
4.5 CONCLUSIONS ON RADIOLOGICAL CONSEQUENCES	4-14
4.6 REFERENCES	4-15
5.0 SUMMARY AND CONCLUSIONS	5-1
APPENDICES:	A.0-1
INDEX TO SENSITIVITY STUDIES IN APPENDICES	A.0-2
A. DEVELOPMENT PROGRAMS SUPPORTING THERMAL MARGIN ASSESSMENTS	A-1
A.1 SODIUM-CONCRETE INTERACTIONS DEVELOPMENT PROGRAM	A-1
A.1.1 Purpose	A-1
A.1.2 Program	A-1
A.1.3 Schedule	A-2
A.1.4 Criteria of Success	A-3
A.1.5 Fallback Position	A-3
A.2 HYDROGEN AUTO-CATALYTIC RECOMBINATION	A-4
A.2.1 Purpose	A-4
A.2.2 Program	A-4
A.2.3 Schedule	A-5
A.2.4 Conclusions	A-5

TABLE OF CONTENTS (Continued)

	<u>Page</u>
A.3 FURTHER VALIDATION OF THE CACECO COMPUTER CODE	A-6
A.3.1 Purpose	A-6
A.3.2 Program	A-6
A.3.3 Schedule	A-6
A.3.4 Conclusions	A-7
A.4 COMPREHENSIVE TESTING PROGRAM FOR CONCRETE AT ELEVATED TEMPERATURES	A-8
A.4.1 Purpose	A-8
A.4.2 Program	A-8
A.4.3 Schedule	A-11
A.4.4 Conclusions	A-12
A.5 BASE MATERIALS TEST FOR LINER STEEL	A-13
A.5.1 Purpose	A-13
A.5.2 Program	A-13
A.5.3 Schedule	A-15
A.5.4 Criteria of Success	A-15
A.5.5 Fallback Position	A-16
A.6 SODIUM SPILL DESIGN QUALIFICATION TEST (LT-1)	A-17
A.7 TMBDB AIR CLEANING SYSTEM PERFORMANCE TESTS	A-18
A.7.1 Purpose	A-18
A.7.2 Program	A-18
A.7.3 Schedule	A-20
A.7.4 Conclusions	A-21
A.8 REFERENCES	A-22
B. REACTOR AND GUARD VESSEL PENETRATION ANALYSIS	B-1
B.1 INTRODUCTION	B-1
B.2 ASSUMPTIONS	B-3
B.3 DESCRIPTION OF PENETRATION ANALYTICAL MODEL	B-5
B.4 DESCRIPTION OF CASES	B-6
B.5 RESULTS	B-9
B.6 CONCLUSIONS	B-12
B.7 REFERENCES	B-13

TABLE OF CONTENTS (Continued)

	<u>Page</u>
C. ANALYTIC THERMAL MODELS AND DATA BASE	C.0-1
C.1 PRE-SODIUM BOILDY MODEL AND DATA BASE	C.1-i
C.1.1 Physical Description	C.1-1
C.1.2 Heat Sources	C.1-3
C.1.3 Heat and Mass Transfer	C.1-5
C.1.4 Material Properties	C.1-8
C.1.5 References	C.1-11
C.2 POST SODIUM BOILDY MODEL AND DATA BASE	C.2-1
C.2.1 Analytical Model	C.2-1
C.2.2 Data Base	C.2-3
C.2.3 References	C.2-5
C.3 STRUCTURAL MATERIAL PROPERTIES AT ELEVATED TEMPERATURES	C.3-1
C.3.1 Introduction	C.3-1
C.3.2 Concrete Properties	C.3-1
C.3.3 Properties of Reinforcing Steel	C.3-11
C.3.4 Properties of Liner Steel	C.3-12
C.3.5 References	C.3-16
D. AEROSOL BEHAVIOR MODEL	D-1
D.1 INTRODUCTION	D-1
D.2 AEROSOL MODELING AND BASES	D-1
D.3 SENSITIVITY TO RCB TEMPERATURE	D-4
D.4 REFERENCES	D-6
E. RELEASE OF PLUTONIUM AND FISSION PRODUCTS	E-1
E.1 INTRODUCTION	E-1
E.2 PLUTONIUM RELEASE FROM SODIUM-OXYGEN REACTIONS IN THE INERTED CELLS	E-1
E.3 PLUTONIUM RELEASE FROM A BOILING POOL OF SODIUM	E-2
E.4 PLUTONIUM RELEASE AFTER SODIUM BOILDY	E-4
E.5 CONCLUSIONS ON PLUTONIUM RELEASE	E-6
E.6 FISSION PRODUCT RELEASE TO THE RCB	E-6
E.7 EFFECT OF CO ₂ REACTION WITH NaOH ON FISSION PRODUCT RELEASE FROM THE RCB	E-8
E.8 REFERENCES	E-10
F. EVALUATION OF ALTERNATE SCENARIOS	F.0-1
F.1 EFFECT OF DECAY HEAT ON THE BASE TMBDB SCENARIO	F.1-1
F.1.1 Introduction	F.1-1
F.1.2 Model Modifications	F.1-1

TABLE OF CONTENTS (Continued)

	<u>Page</u>
H.2 FLAME LENGTHS FOR TMBDB SCENARIO	H.2-1
H.2.1 Introduction	H.2-1
H.2.2 Flame Length Calculation	H.2-2
H.2.3 Effects on Containment	H.2-6
H.2.4 Conclusions	H.2-8
H.2.5 References	H.2-9
H.2.A Flame Length Correlation	H.2-16
H.3 POTENTIAL FOR HYDROGEN STRATIFICATION	H.3-1
H.3.1 Introduction	H.3-1
H.3.2 Pre-Hydrogen Ignition Time Period	H.3-1
H.3.3 Hydrogen Ignition to Sodium Boildry Time	H.3-4
H.3.4 Post Sodium Boildry	H.3-4
H.3.5 Conclusions	H.3-5
H.3.6 References	H.3-5
I. ASSESSMENT OF CONSEQUENCES OF FUEL IN PHTS PIPING FOLLOWING REACTOR VESSEL DRAINING	I-1
I.1 INTRODUCTION	I-1
I.2 EFFECT ON PHTS PIPING	I-3
I.3 EFFECT ON CELL LINERS	I-5
I.4 SENSITIVITY ASSESSMENT OF FUEL IN PHTS PIPING	I-7
J. NRC'S REQUESTS FOR ADDITIONAL INFORMATION (RAI's) ON CORE MELTDOWN CONSIDERATIONS	J-1

LIST OF TABLES

<u>Table Number</u>		<u>Page</u>
2-1	CRBRP FEATURES PROVIDING THERMAL MARGIN BEYOND THE DESIGN BASE	2-42
3-1	PUMP COASTDOWN DATA	3-76
3-2	PARTICULE DISTRIBUTION FOLLOWING IN-VESSEL SETTLING	3-77
3-3	DISTRIBUTION OF UPWARD EJECTED DEBRIS	3-78
3-4	PARTICLE DRAG COEFFICIENTS	3-79
3-5	MAXIMUM CRBR FULL EQUILIBRIUM CYCLE DECAY POWER BY REGION	3-80
3-6	STABLE DEBRIS BED DEPTHS	3-81
3-7	COMPARISON OF FUEL RETENTION CAPABILITY WITH PREDICTED FUEL DISTRIBUTION	3-82
3-8	SENSITIVITY OF CONTAINMENT PARAMETERS AT 24 HOURS AFTER AN HCDA TO VESSEL PENETRATION TIME	3-83
3-9	ANNULUS COOLING SYSTEM ANALYSIS DATA	3-84
3-10	CONTAINMENT STRUCTURAL CAPABILITY	3-85
3-11	$K_{\text{effective}}$ OF VARIOUS GEOMETRIES	3-86
3-12	REACTOR CAVITY AND PIPEWAY CELL LINER FAILURE TIMES	3-87
3-13	HEAT TRANSFER COEFFICIENT USED IN THERMAL ANALYSIS OF THE REACTOR CAVITY LEDGE	3-88
3-14	SUMMARY OF RESULTS FOR SUBMERGED LINER (WITHOUT CREEP)	3-89
3-15	SUMMARY OF RESULTS FOR LINER ABOVE SODIUM POOL (WITHOUT CREEP)	3-90
4-1	CORE SOURCE TERMS RELEASED TO THE REACTOR CONTAINMENT BUILDING FOR HYPOTHETICAL ACCIDENT SCENARIOS CONSIDERED	4-17
4-2	ATMOSPHERIC DILUTION FACTORS	4-18
4-3	DOSE SUMMARY FOR HYPOTHETICAL ACCIDENT SCENARIOS CONSIDERED	4-19

LIST OF TABLES (Continued)

<u>Table Number</u>		<u>Page</u>
F.7-1	EFFECTS OF PIPEWAY FLOOR LINER FAILURE ON CONTAINMENT CONDITIONS AT 24 HOURS	F.7-4
F.7-2	EFFECTS OF PIPEWAY FLOOR LINER FAILURE ON CONTAINMENT CONDITIONS AT 30 HOURS	F.7-5
F.7-3	EFFECTS OF PIPEWAY FLOOR LINER FAILURE ON CONTAINMENT CONDITIONS AT 36 HOURS	F.7-6
F.7-4	EFFECTS OF PIPEWAY FLOOR LINER FAILURE ON CONTAINMENT CONDITIONS AT 50 HOURS	F.7-7
F.7-5	EFFECTS OF PIPEWAY FLOOR LINER FAILURE ON CONTAINMENT CONDITIONS AT BOILDRY	F.7-8
F.7-6	DEPENDENCE OF PEAK CONTAINMENT CONDITIONS TO SODIUM BOILDRY ON PIPEWAY FLOOR LINER FAILURE ASSUMPTIONS	F.7-9
F.7-7	SUMMARY OF CONTAINMENT CONDITIONS FOR "LESS SEVERE" LINER FAILURE SENSITIVITY ANALYSES	F.7-15
G.1-1	ASSESSMENT OF POTENTIAL FOR BED DRYOUT IN THE REACTOR CAVITY	G.1-7
G.2-1	SUMMARY OF SENSITIVITY STUDIES ON SODIUM-CONCRETE REACTIONS	G.2-4
G.3-1	SENSITIVITY OF RCB AND RC CONDITIONS AT 24 HOURS TO RC VENT FAILURE MODES	G.3-4
G.4-1	EFFECT OF INITIAL FUEL, FISSION PRODUCT, AND SODIUM RELEASE	G.4-4
G.4-2	EFFECT OF INITIAL FUEL AND FISSION PRODUCT RELEASE WITH SODIUM RELEASE FIXED AT 1000 LB.	G.4-5
G.4-3	EFFECT OF SODIUM RELEASE FOR A GIVEN 10% FUEL-FISSION PRODUCT RELEASE	G.4-6
H.1-1	CONTAINMENT ATMOSPHERE CONDITIONS AT 24 HOURS	H.1-10
H.3-1	ATMOSPHERIC ENTRAINMENT IN HYDROGEN JET	H.3-6
I-1	DISTRIBUTION OF UPWARD EJECTED DEBRIS FOR LOF HCDA	I-8
I-2	HEAT GENERATION AS A FUNCTION OF TIME FOR TOTAL CORE AND BLANKETS	I-9
I-3	PARAMETERS FOR PIPE MELTING ANALYSIS	I-10
I-4	FLOOR PENETRATION ANALYSIS PARAMETERS	I-11

LIST OF FIGURES

<u>Figure Number</u>		<u>Page</u>
1-1	Design Features Providing Thermal Margin Beyond the Design Base	1-6
2-1	Maximum Pressure Differential Between the Reactor Cavity and Head Access Area	2-43
2-2	Maximum Reactor Cavity Atmosphere Pressure	2-44
2-3	Maximum Reactor Cavity Atmosphere and Sodium Pool Temperature	2-45
2-4	Maximum Pressure Differential Between the Reactor Cavity and Cell 105	2-46
2-5	Maximum Containment Atmosphere Temperature	2-47
2-6	Maximum Containment Atmosphere Pressure	2-48
2-7	Maximum Containment Vent Rates	2-49
2-8	Maximum Heat Load Through the Containment Structure Steel Shell	2-50
2-9	Maximum Reactor Cavity Submerged Wall Structural Temperatures	2-51
2-10	Maximum Reactor Cavity Floor Concrete Temperatures	2-52
2-11	Maximum Reactor Cavity Non-Submerged Wall Structural Temperatures	2-53
2-12	Maximum Reactor Cavity-Pipeway Wall Structural Temperatures	2-54
2-13	Maximum Pipeway Cell Wall Structural Temperatures (2.5 Ft. Thick Wall)	2-55
2-14	Maximum Pipeway Floor Structural Temperatures	2-56
2-15	Maximum Pipeway Cell Wall Structural Temperatures (4.0 Ft. Thick Wall)	2-57
2-16	Maximum Pipeway Cell Roof and Head Access Area Wall Structural Temperatures	2-58
2-17	Reactor Cavity Ledge Radial Temperature Profile	2-59

LIST OF FIGURES (Continued)

<u>Figure Number</u>		<u>Page</u>
2-18	Reactor Cavity Ledge Axial Temperature Profile	2-60
2-19	Maximum Reactor Cavity Upper Wall Temperatures Prior to Wall Failure	2-61
2-20	Maximum Reactor Cavity Lower Wall Temperatures Prior to Wall Failure	2-62
2-21	Maximum Reactor Cavity Floor and Basemat (Axial Centerline) Temperatures	2-63
2-22	Maximum Reactor Cavity Floor (Elevation 733.5) Temperatures	2-64
2-23	Maximum Basemat (Elevation 728.0) Temperatures	2-65
2-24	Maximum Basemat (Elevation 718.0) Temperatures	2-66
2-25	Maximum PHTS Wall (Facing RC Wall) Temperatures	2-67
2-26	Maximum PHTS Wall (Not Facing RC Wall) Temperatures	2-68
2-27	Maximum Containment Wall Temperatures (Below Elevation 816.0)	2-69
2-28	Maximum Confinement Wall Temperatures (Below Elevation 816.0)	2-70
2-29	Maximum Temperatures of Wall Separating Cells 102 and 105	2-71
2-30	Maximum Operating Floor Temperature	2-72
2-31	Location of Post Boildry Temperature Profile Plots	2-73
2-32	Guard Vessel Skirt Support Detail	2-74
2-33	Reactor Cavity Vent System	2-75
2-34	Containment Vent, Purge and Cleanup Systems	2-76
2-35	CRBRP Containment TMBDB Instrumentation	2-77
2-36	Atmospheric Temperatures for Determining Containment Penetrations Environment (Beyond 100 Hours)	2-78
3-1	10 x 11 Array VARR-II Outlet Plenum Model with Complex UIS Geometry	3-91

LIST OF FIGURES (Continued)

<u>Figure Number</u>		<u>Page</u>
3-2	Simplified Drawing of Settling in Horizontal Pipes	3-92
3-3	Particle Size Distributions From Large-Scale Out-of-Pile Tests	3-93
3-4	Hydrogen Burning Criterion	3-94
3-5	CACECO Code Containment Model	3-95
3-6	Reactor Cavity and Containment Atmosphere and Containment Steel Dome Temperatures	3-96
3-7	Reactor Cavity and Containment Pressures	3-97
3-8	Sodium Entering Containment From the Reactor Cavity	3-98
3-9	Integrated Water Release from Concrete Structures	3-99
3-10	Sodium Concentration Entering Containment	3-100
3-11	Containment Building Hydrogen Concentration	3-101
3-12	Containment Oxygen Concentration	3-102
3-13	Gases Leaving Containment	3-103
3-14	Air Purge Rate into Containment	3-104
3-15	Total RCB Sodium Oxide and Sodium Hydroxide Inventory (Neglecting Aerosol Leakage)	3-105
3-16	Reactor Cavity Submerged Wall Concrete Temperatures	3-106
3-17	Reactor Cavity Floor Concrete Temperatures	3-107
3-18	Reactor Cavity Non-Submerged Concrete Wall Temperatures	3-108
3-19	Reactor Cavity - Pipeway Wall Concrete Temperatures	3-109
3-20	Pipeway Cell Wall Structural Temperatures (2.5 Ft. Thick Wall)	3-110
3-21	Pipeway Cell Wall Structural Temperatures (4.0 Ft. Thick Wall)	3-111

LIST OF FIGURES (Continued)

<u>Figure Number</u>		<u>Page</u>
H.1-6	Flammability Limits for Predicted Scenario and Hydrogen Burning Scenario that Bounds Containment Pressure and Temperature	H.1-16
H.1-7	Effect of Hydrogen Burning Assumptions on Containment Atmosphere Temperatures (Without Containment Venting and Purging)	H.1-17
H.1-8	Effect of Hydrogen Burning Assumptions on Containment Atmosphere Pressure (Without Containment Venting and Purging)	H.1-18
H.1-9	Effect of Hydrogen Burning Assumptions on Containment Atmosphere Hydrogen Concentration (Without Containment Venting and Purging)	H.1-19
H.1-10	Effect of Hydrogen Burning Assumptions on Containment Conditions with Respect to Flammability Limits (Without Containment Venting and Purging)	H.1-20
H.2-1	Flow Patterns in Laminar and Turbulent Flames	H.2-10
H.2-2	TMBDB Mass Flow Rate Through the Reactor Cavity to RCB Vent	H.2-11
H.2-3	Dependence of Flame Length on Nozzle Diameter	H.2-12
H.2-4	Multiple Nozzle Arrangement	H.2-13
H.2-5	Dependence of Flame Length on Number of Nozzles (0.7853 FT ² Total Area)	H.2-14
H.2-6	Temperatures on Axis of a Hydrogen Diffusion Flame (Burner Diameter = 4 Inches, Flow Rate = 3.5 CFM)	H.2-15
H.2.A-1	Flame Length Correlation (Figure 255 of Ref. H.2-1)	H.2-18
H.2.A-2	Effect of Nozzle Velocity on Flame Length (Figure 246 of Ref. H.2-1)	H.2-19
H.3-1	Flow Patterns for Jet Injection Into a Closed Container	H.3-7
I-1	PHTS Pipe and Insulation Configuration	I-12
I-2	Peak Pipe Temperature versus Fuel Content	I-13
I-3	Sketch of Fuel Debris In Pipe	I-14
I-4	Cell Liner Thermal Model Schematic	I-15
I-5	Liner Mid-Plane Peak Temperature versus Fuel Density	I-16

ABBREVIATIONS

ANL	Argonne National Laboratory
ARD	Advanced Reactors Division (of Westinghouse Electric Corporation)
ASME	American Society of Mechanical Engineers
ATWS	Anticipated Transients Without Scram
BOEC	Beginning of Equilibrium Cycle
BOL	Beginning of Life
CAM	Continuous Air Monitors
CFR	Code of Federal Regulation
CRBR	Clinch River Breeder Reactor
CRBRP	Clinch River Breeder Reactor Plant
CRDM	Control Rod Drive Mechanism
CSS	Core Support Structure
DHRS	Direct Heat Removal Service
DOE	U. S. Department of Energy
EOEC	End of Equilibrium Cycle
ERDA	U.S. Energy Research and Development Administration
ESF	Engineered Safety Features
FMEA	Failure Mode and Effects Analysis
FFTF	Fast Flux Test Facility
FWP	Feedwater Pump
GE	General Electric Company
HAA	Head Access Area
HCDA	Hypothetical Core Disruptive Accident
HEDL	Hanford Engineering Development Laboratory
HEPA	High Efficiency Particulate Air
HTS	Heat Transport System
HVAC	Heating, Ventilating and Air Conditioning
IEEE	Institute of Electrical and Electronic Engineers
IHTS	Intermediate Heat Transport System
IHX	Intermediate Heat Exchanger
IMAS	Impurity Monitoring and Analysis System
IRP	Intermediate Rotating Plug
IVTM	In-Vessel Transfer Machine

2. To insure containment atmosphere mixing before venting, the purge air shall be injected into containment below elevation 840'.
3. The purge system shall prevent backflow from containment to the outside atmosphere.
4. The purge system, in combination with the containment vent and cleanup systems, shall maintain containment at a negative pressure after the containment pressure is reduced by the initial venting after 24 hours.
5. The purge system operations shall be by remote manual actuation from the control room.

2.1.2.8 Containment Vent System

1. To prevent containment failure by excessive pressure, the vent system shall have a capacity between 24,000 and 26,400 acfm with a containment pressure of 30 psia, a containment atmosphere density of 0.07 lb/ft³ and a viscosity of 0.06 lb/ft-hr. It shall remain functional if up to 300,000 pounds of aerosol enter the system at a maximum rate of 5,600 lb/hr.
2. The vent system shall exhaust the containment atmosphere from the containment into the containment cleanup system.
3. The containment vent system shall be compatible with the following gases, vapors and aerosols: Ar, N₂, H₂, H₂O, CO, CO₂, O₂, Na₂O, Na₂O₂, NaOH, Na₂CO₃, fission products, and compounds resulting from fission product reactions. The system must remain functional for inlet gas temperatures and pressures given on Figures 2-5 and 2-6, and, beyond 150 hours for temperatures up to 250°F.
4. The vent system operations shall be by remote manual actuation from the control room.

2.1.2.9 TMBDB Containment Cleanup System

1. The containment cleanup system efficiency shall be a minimum of 99% for vented materials in the solid or liquid state, 97% for vapors (NaI, SeO_2 , and Sb_2O_3) subject to condensation in the cleanup system, and 0% for noble gases. These efficiencies shall apply when subjected to the vent rates on Figure 2-7 and containment atmosphere temperatures on Figure 2-5 with a containment atmosphere density of 0.07 lb/ft^3 ; beyond 150 hours, containment atmosphere temperatures up to 250°F shall apply. It shall be capable of performing all of its intended functions in the presence of Ar, N_2 , H_2 , H_2O , CO, CO_2 , O_2 , Na_2O , Na_2O_2 , NaOH, Na_2CO_3 , fission products, and compounds resulting from fission product reactions.
2. The containment cleanup system shall remain functional at an aerosol mass flow rate of up to 5,600 lb/hr and a total mass of 300,000 pounds of aerosol entering the cleanup system. The principal constituents of the aerosol are NaOH and Na_2O , the proportions of which can vary from 0 to 100% of the aerosol, and Na_2CO_3 which can vary from 0 to 8% of the aerosol.

The aerosol particle properties are:

Mass Mean Radius (microns):	$5 < r_{50} < 10$
Aerodynamic Equivalent Radius (microns):	$2.3 < \text{AER} < 4.7$
Density (g/cc):	$2.1 < \rho < 2.5$
Mass Geometric Standard Deviation:	$3.0 < \sigma < 3.5$

Aerodynamic equivalent radius is based on $\text{AER} = r_{50} (\rho\alpha)^{0.5}$

where $\rho = 2.21$ and $\alpha = 0.1$

3. The containment cleanup system shall remain functional at fission products power levels in the accumulated filter aerosol of:

Time (hours)	Fission Product Power (MW)
0	0
24	3.1×10^{-5}
48	0.16*
96	0.16*
240	0.11
720	0.05

4. The containment cleanup system design shall be capable of performing all its intended functions with the following chemical and physical states of the 10 most radiologically significant fission products in the containment atmosphere:

*Maximum value.

MAXIMUM PERCENTAGE OF THE FISSION PRODUCTS BY CHEMICAL AND PHYSICAL FORM

Element	Elemental		Oxide	
	Vapor	Liquid or Solid	Vapor	Liquid or Solid
Se	1%	1%	100%	100%
Rb	1	1	1	100
Sr	1	1	1	100
Zr	1	1	1	100
Sb	1	1	100	100
Te	1	1	1	100
Cs	1	1	1	100
Ba	1	1	1	100
Ce	1	1	1	100
I	1	1	33	100

NaI

5. The exhaust from the containment cleanup system shall have a temperature compatible with operation of the TMBDB Exhaust-Plant Effluent Radiation Monitoring System.
6. The containment cleanup system operations shall be by remote manual actuation from the control room.

| 1

2.1.2.10 Annulus Cooling System

1. To insure containment and confinement do not fail from excessive temperatures, the annulus cooling system shall remove the heat load into the containment steel shell on Figure 2-8.
2. Steel containment temperatures shall be below those that cause structural failure or excessive containment leakage.
3. Concrete confinement temperatures shall be below those that cause structural failure.
4. The annulus cooling system operations shall be by remote manual actuation from the control room.

| 1

2.1.2.11 Containment System Leakage Barrier

At any given time, containment out-leakage shall not exceed the greater of:

| 4

1. The design leakrate (0.1 volume percent per day).
2. The design leakrate adjusted for pressures above the containment design pressure of 10 psig. $\text{Leakrate} = \text{Design Leakrate} \times (\text{Actual Pressure (psig)})^{.5/3.2}$.

All containment penetrations, including fluid systems piping and containment isolation valves, electrical penetrations, and hatches, shall maintain their integrity such that the above leakages are not exceeded for at least 100 hours following the initiation of the TMBDB scenario. The limiting TMBDB temperature, pressure and radiation environmental requirements for penetrations during the 100 hours period shall be as follows:

CONTAINMENT PENETRATIONS ENVIRONMENT (0-100 HOURS)

<u>Containment Penetration Location</u>	<u>Maximum Temperature (°F)</u>	<u>Maximum Pressure</u>	<u>Peak Radiation Level (R/hr)</u>	<u>Total Accumulated Dose (R)</u>
PHTS Cells	250	Figure 2-6	1×10^6	3×10^6
RCB Above Operating Floor	Figure 2-5	Figure 2-6	1×10^6	1×10^7
All Other Cells	250	Figure 2-6	1×10^6	3×10^6

After containment venting/purging is initiated (24 to 100 hours), containment in-leakage shall not exceed 1000 scfm at a negative pressure inside of -3.5 inches water.

The limiting TMBDB temperature, pressure and radiation environmental requirements for containment penetrations after 100 hours are as follows:

CONTAINMENT PENETRATIONS ENVIRONMENT (Beyond 100 Hours)

<u>Containment Penetration Location</u>	<u>Maximum Temperature (°F)</u>	<u>Minimum Pressure (In. Water)</u>	<u>Peak Radiation Level (R/hr)</u>	<u>Total Accumulated Dose (R)</u>
PHTS Cells	Figure 2-36	-3.5	5×10^3	1×10^7
RCB Above Operating Floor	Figure 2-5*	-3.5	1×10^5	1×10^8
All Other Cells	Figure 2-36	-3.5	5×10^3	1×10^7

*Beyond 150 hours, the maximum temperature is 250°F. Figure 2-5 defines the atmosphere temperatures. The designer shall determine the appropriate penetration temperature that would result from the atmosphere temperatures. Figures 3-27 and 3-28 provide selected steel shell temperatures that can also be used for this determination.

Containment penetrations above the operating floor shall perform their function in the presence of the following plated sodium aerosol (including NaOH, Na₂O, and Na₂CO₃):

Vertical Surfaces: 0.5 lb/ft²
Horizontal Surfaces: 80 lb/ft²

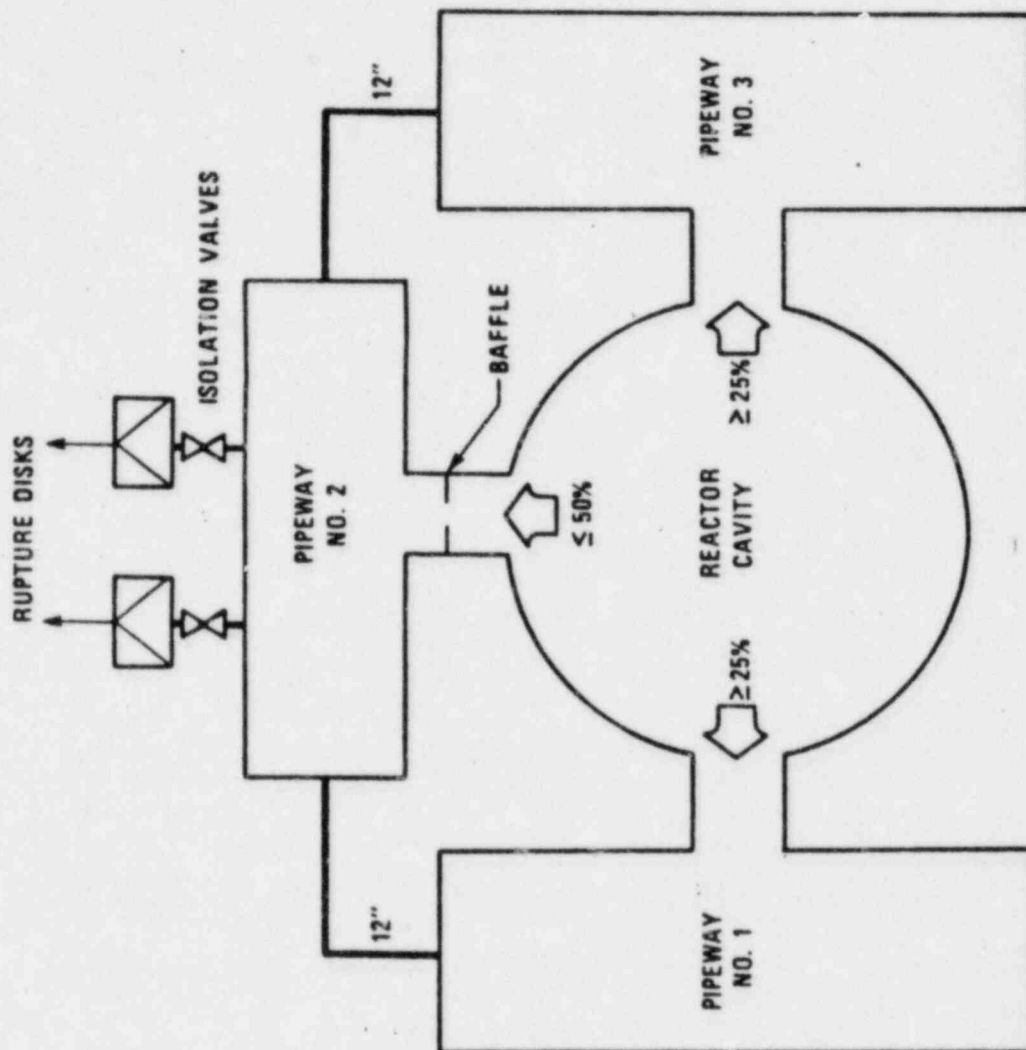
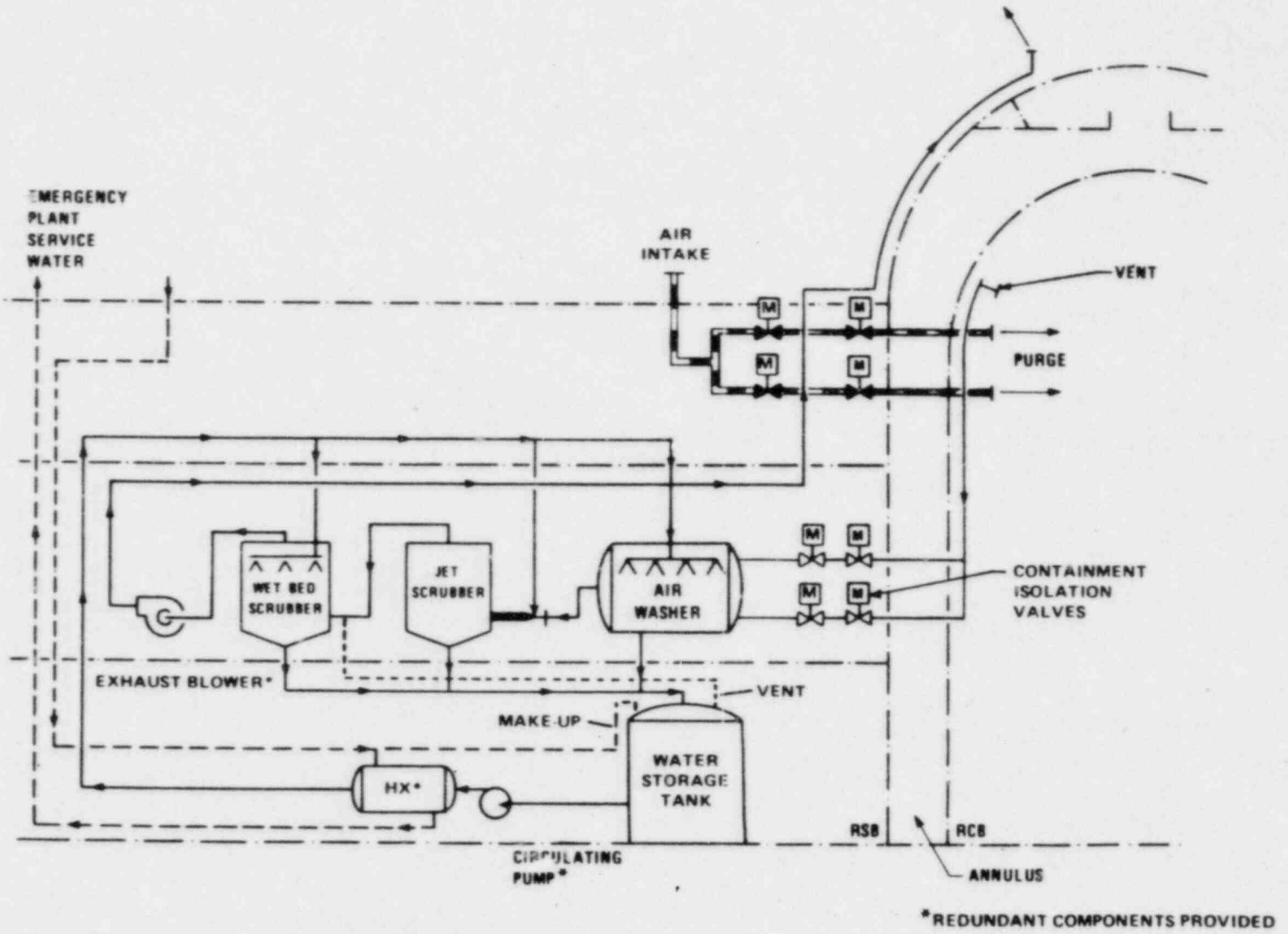


Figure 2-33 Reactor Cavity Vent System

1966-33

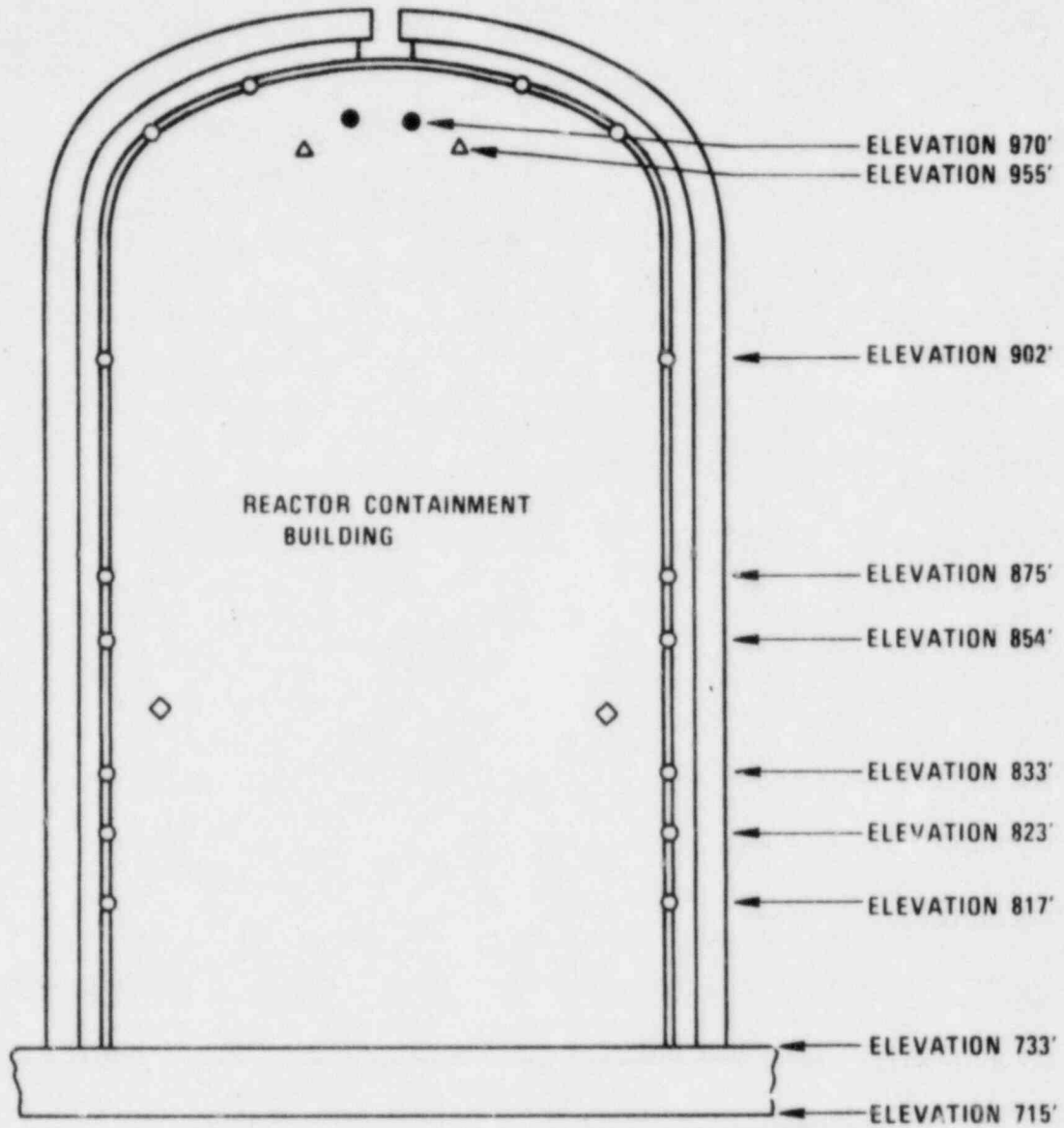
7184-3



2-76

CRBRP-3
Vol. 2, Rev. 4

Figure 2-34. Containment Vent, Purge and Cleanup Systems



KEY

- HYDROGEN MEASUREMENT SYSTEM SAMPLE POINTS
- REACTOR CONTAINMENT VESSEL TEMPERATURE
- △ REACTOR CONTAINMENT ATMOSPHERE TEMPERATURE
- ◇ REACTOR CONTAINMENT PRESSURE

Figure 2-35 CRBRP Containment TMBDB Instrumentation

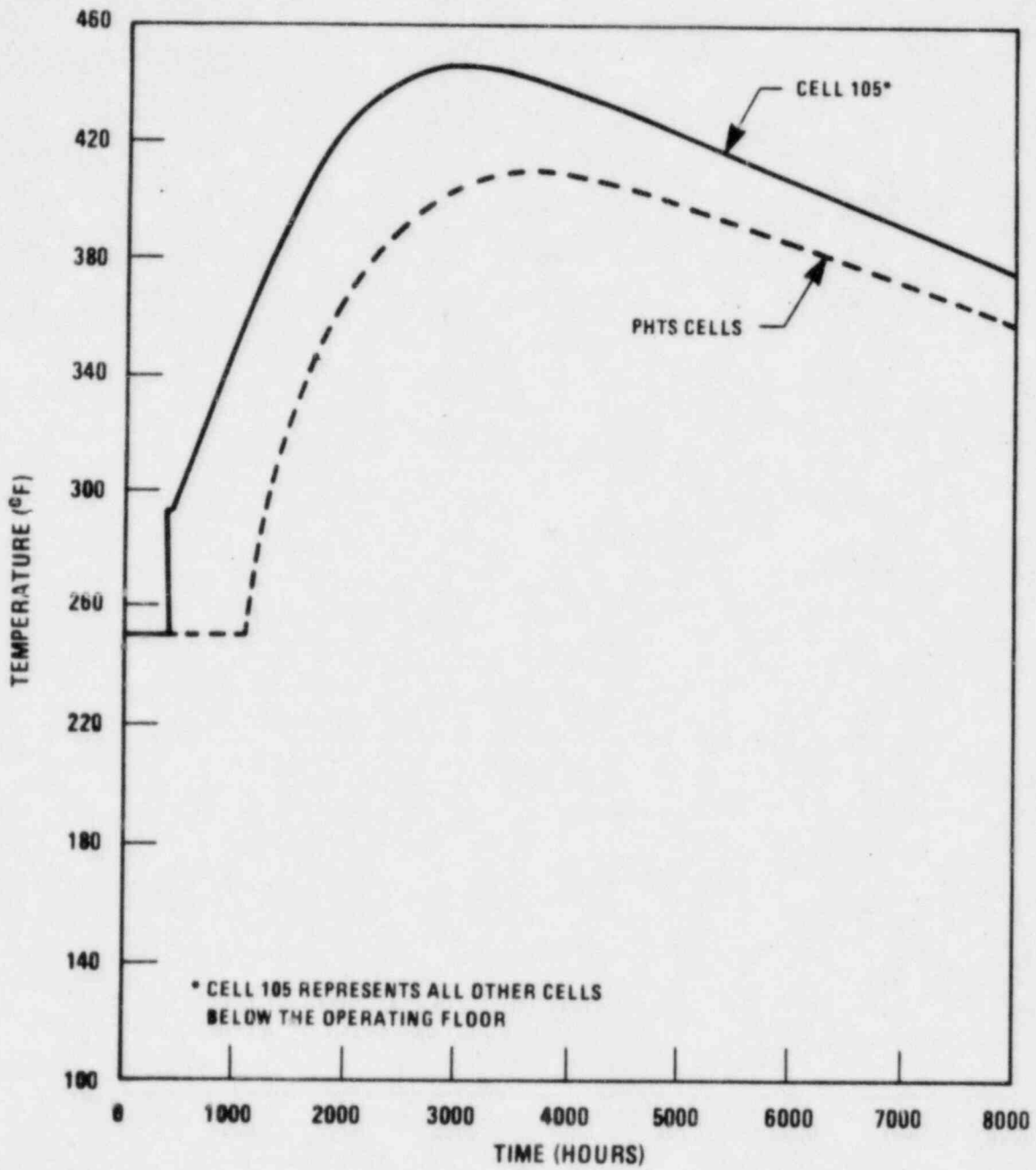


Figure 2-36. Atmospheric Temperatures for Determining Containment Penetrations Environment (Beyond 100 Hours)

7184-1

Criteria for hydrogen burning:

- a. The hydrogen-nitrogen mixture entering containment is above 1450°F.
- b. The hydrogen-sodium-nitrogen mixture entering containment contains at least 6 g/m³ of sodium at temperatures above 500°F.
- c. The oxygen concentration is above 8%. With the oxygen concentration above 5% and the hydrogen concentration above 4%, the hydrogen in excess of 4% would burn. Figure 3-4 illustrates this burning criterion.

Criterion (a) is not met for the analyses reported herein. The sodium concentration entering the reactor containment building would satisfy criterion (b) after about ten hours following vessel penetration. At the end of this time the hydrogen concentration in containment would reach approximately 4.5%. This hydrogen would burn while the burning criteria are satisfied as the natural circulation in containment moves the hydrogen through the flame. The oxygen concentration is predicted to remain above 8% (satisfying criterion c) for 36 hours; thus, no hydrogen accumulation would occur during this time (i.e. 10 to 36 hours).

The flame characteristics are shown in Appendix H.2 to be such that excessive local containment steel temperatures would not occur.

When hydrogen burning criteria are no longer satisfied, hydrogen would accumulate in the containment. The hydrogen concentration would be controlled to less than 6% by purging (see item 17). Since the

hydrogen concentration is maintained well below explosive levels, the containment integrity would not be challenged by hydrogen reactions.*

14. Water vapor from concrete in the operating floor and head access area would enter the containment atmosphere.

The sodium oxide created by the sodium-oxygen, sodium-carbon dioxide, and sodium-water reactions in containment would react with the excess water vapor in the containment atmosphere to form sodium-hydroxide.

15. The maximum containment pressure of 22 psig (peak pressure results from assumption that accumulated hydrogen burns instantly) is well below the failure pressure. Scoping calculations indicate that the failure pressure is in excess of 30 psig for these conditions (see Table 3-10).
16. At 36 hours the annulus cooling system is assumed to be activated to maintain the containment temperature at an acceptable level and the containment is vented to avoid excessive long term pressure and to allow a purge of fresh air to be initiated.

*Appendix H.3 considers the potential for a high concentration of the lighter hydrogen collecting at the top of the RCB due to buoyancy forces (stratification). It is concluded that in the TMBDB scenario the mixing forces would be more than adequate to counteract buoyancy forces and to prevent any significant collection (stratification) of hydrogen at the top of the RCB.

Dose Factors

Dose conversion factors (rem/ci) used in the COMRADEX code to calculate specific organ doses were taken from References 4-8 and 4-9 where possible. Factors for isotopes not given in these References are from Reference 4-10.

Containment Modeling

The time dependent radiological source term is released directly to the RCB. The release rate from the RCB is that calculated by the CACECO code. For the first 36 hours of the scenario the RCB atmosphere leaks at a low rate (based on 0.1%/day at 10 psig) to the annulus filter system (described in Section 6.2.5 of the PSAR). During this 36 hour period unfiltered bypass leakage at the rate of 1% of the filtered leakage is considered. After 36 hours the RCB is vented and subsequently purged (Figures 3-13 and 3-14) to maintain the hydrogen concentration at an acceptable level. During this phase filtering is by the TMBDB filter system which is designed for the higher vent rates. The efficiency of the TMBDB filter system is 99% for solid fission products and fuel and 97% for condensible fission products (halogens, Se, and Sb). Noble gases are assumed to pass through the filter system unattenuated. (There is some question of the effectiveness of the filter system to remove Na_2CO_3 and the fission products which may be tied up with this aerosol component. This subject is addressed in Appendix E.) Because the bypass leakage rate is expected to be so small relative to the high vent rate after 36 hours, the bypass leakage is not expected to make a significant contribution to the released radioactivity and is therefore not considered beyond 36 hours.

The direct gamma contribution to the whole body dose considers the shielding provided by the steel RCB and the concrete confinement building.

Figure 4-1 shows the dose rate inside the reactor containment building for Case 2.

4.2.2 Radiological Doses

Using the methods described in Section 4.2.1 the radiological doses at the Exclusion Boundary (0.42 miles) and the Low Population Zone (2.5 miles) were calculated for the four different source terms described in Section 4.1. These doses are summarized in Table 4-3. The 30 day LPZ doses include the plutonium released after boil-dry to 30 days. Plutonium release beyond 30 days could result in an additional 10 rem to the LPZ bone dose. Control room doses were provided in Section 2.2.15.

The dose consequences of the four cases that assumed varying degrees of severity of the hypothetical accident are all quite low for accidents beyond the design base. For example, the maximum whole body dose is predicted to be about 3.5 rem and the maximum thyroid dose would be about 100 rem. Bone doses are about 55 rem.

The results also show that the consequences are not strongly sensitive to the degree of severity of the initial release source term. As the initial release to the RCB increases, the rate of aerosol depletion increases which acts as an inverse feedback to limit the release from the RCB. Consequently, so long as the initial release does not result in failure of the containment barrier, the radiological consequences are relatively insensitive to the magnitude of the release. For the full range of releases considered in Cases 1 through 4, the RCB pressure and temperatures would not result in failure of the containment barrier.

Table 4-4 compares the consequences, in terms of curies released, of a comparable scenario (core meltdown with enough containment leakage to prevent containment failure by overpressure) for CRBRP and light water reactors (LWR). The CRBRP values are for the worst of the above four cases. The LWR releases are for the accident scenarios PWR-6 and BWR-4 described in Section 2 of Appendix VI of WASH-1400. This comparison shows the atmospheric releases for CRBRP to be comparable to those for LWRs. Figure 4-2 shows the integrated radioactivity released to the environment for Case 2.

TABLE 4-3

DOSE SUMMARY FOR HYPOTHETICAL ACCIDENT
 SCENARIOS CONSIDERED

		Doses in REM			
	<u>Organ</u>	<u>Case 1</u>	<u>Case 2</u>	<u>Case 3</u>	<u>Case 4</u>
2 Hour Exclusion Boundary	Bone	0.0043	0.028	0.93	3.83
	Lung	0.0035	0.0055	0.15	0.39
	Thyroid	0.0067	0.0096	11.3	9.51
	W. Body	0.16	0.16	0.24	0.32
30 Day Low Population Zone	Bone	55.1	55.1	55.7	56.2
	Lung	3.95	3.96	3.02	3.02
	Thyroid	99.2	99.2	5.31	1.72
	W. Body	3.51	3.50	3.07	2.94

4

TABLE 4-4

COMPARISON OF RADIONUCLIDE RELEASES TO ATMOSPHERE FOR CRBRP
WITH LWR'S FOR A COMPARABLE MELTDOWN SCENARIO

Element	Radioactivity Released (curies)		
	CRBRP	PWR(3)	BWR(3)
Xe-Kr	2.4×10^7	1.0×10^8	2.1×10^8
I	1.6×10^5	2.0×10^6	1.1×10^6
Cs, Rb	5.4×10^0	1.2×10^4	7.6×10^4
Te, Sb	3.5×10^4	2.2×10^5	8.6×10^5
Ba, Sr	6.5×10^2	3.3×10^4	2.2×10^5
Ru(1)	1.5×10^3	3.9×10^4	3.3×10^5
La(2)	3.7×10^3	2.9×10^4	2.9×10^5

(1) Includes: Ru, Rh, Co, Mo, Te

(2) Includes: Y, La, Zr, Nb, Ce, Pr, Nd, Np, Pu, Am, Cm

(3) From WASH-1400 Appendix VI, Calculation of Reactor Accident Consequences, October 1975. The LWR scenarios used for comparison here are PWR-6 and BWR-4 described in Section 2 of WASH-1400 Appendix VI.

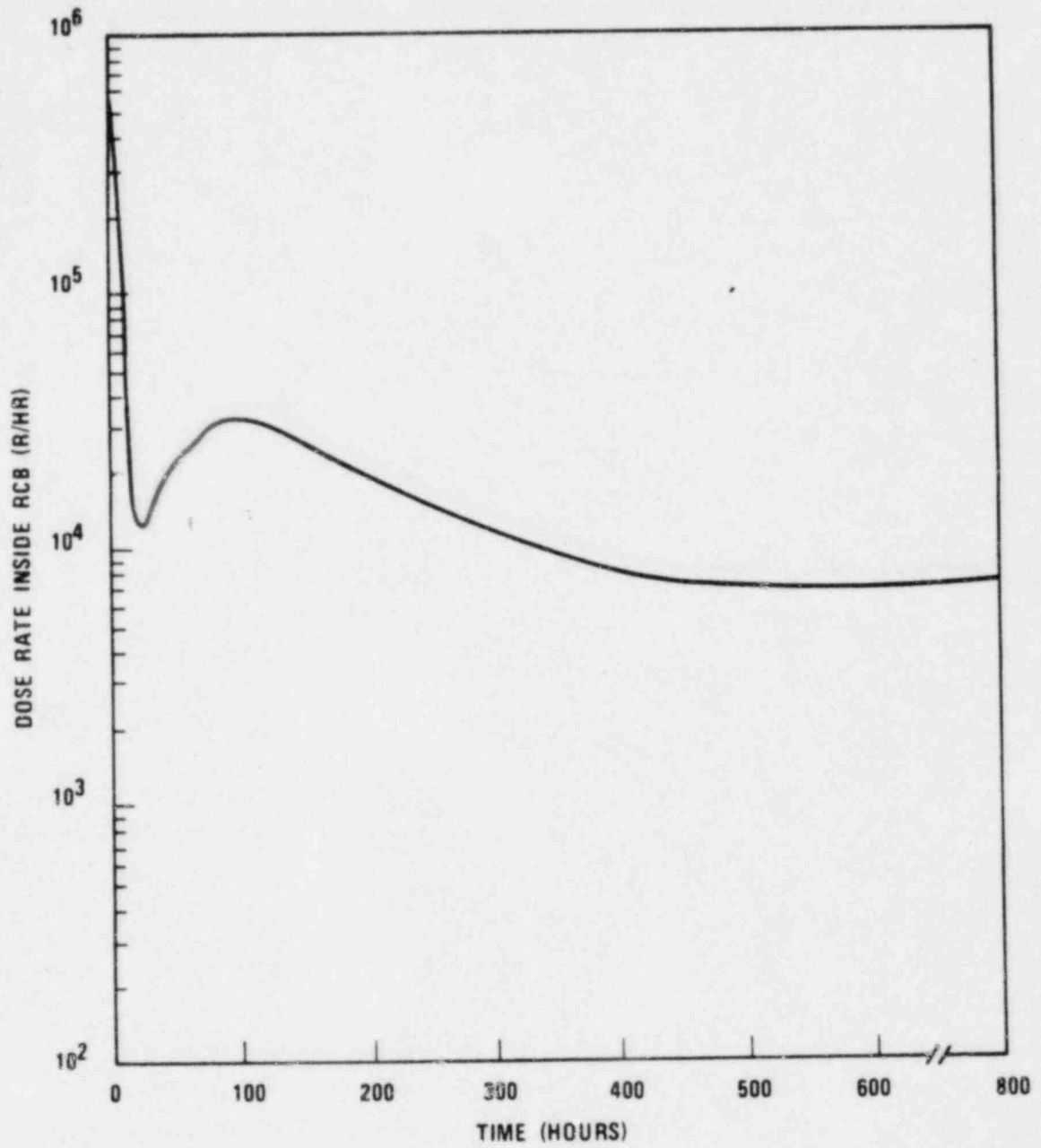


Figure 4-1 Dose Rate Inside the Reactor Containment Building for Case 2

3379-2

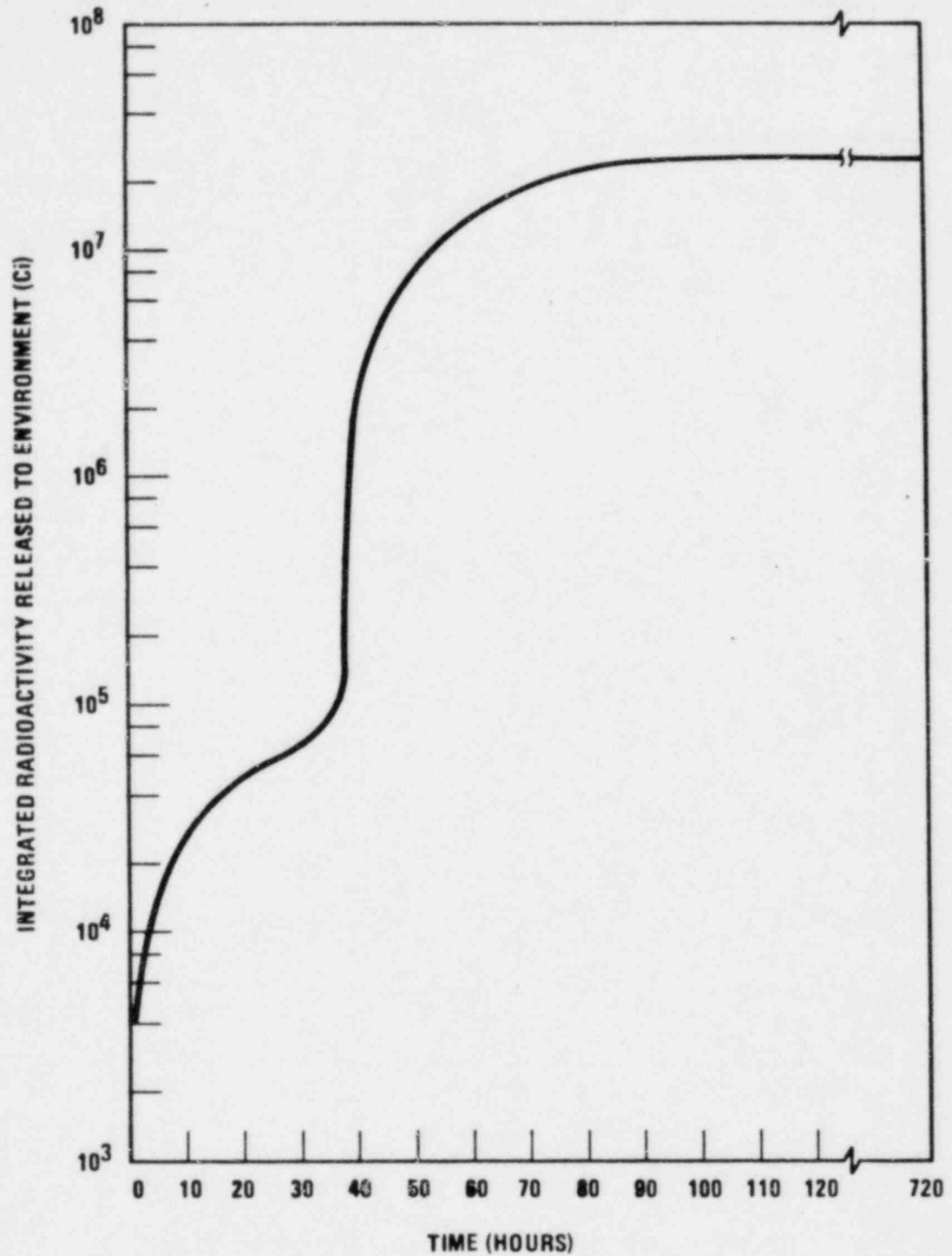


Figure 4-2. Integrated Radioactivity Released to Environment for Case 2

7308-1

APPENDIX A
DEVELOPMENT PROGRAMS SUPPORTING THERMAL MARGIN ASSESSMENTS

This appendix describes the development programs completed and the remaining experimental work scheduled to complete support of TMBDB analyses.

| 4

A.1 SODIUM-CONCRETE INTERACTIONS DEVELOPMENT PROGRAM

A.1.1 Purpose

The large number of sodium-concrete interaction experiments performed at HEDL and Sandia (Appendix C.1, and References A-1 through A-3) resulted in the model of this phenomenon used in the analysis in Section 3.2.2. These tests included both bare concrete and simulated faulted liners. The sodium-concrete experimental program objective has been to increase the experimental data base, to confirm the self-limiting nature of sodium-limestone concrete interactions and to further understand the underlying phenomena involved.

| 4

A.1.2 Program

Two additional large scale sodium-concrete reaction tests have been performed.

| 4

A Large Sodium-Concrete Test (designated LSC-2) has been performed with bare concrete. The test specimen had an interaction surface of 3 feet by 3 feet and used limestone concrete prototypic of CRBRP. The specimen was approximately 2 feet thick. Approximately 1000 pounds of hot ($\sim 1100^{\circ}\text{F}$) sodium was poured onto the test specimen and heated to approximately 1600°F and maintained near this temperature for about 100 hours.

A Large-Scale Faulted Liner Feature Test (designated LFT-6) has also been performed with a steel liner and a layer of MgO gravel above the concrete specimen. The liner contained a 6 inch diameter centered hole. The concrete specimen was similar to that described above for the LSC-2 test.

Approximately 1000 pounds of hot ($\sim 1100^{\circ}\text{F}$) sodium was poured onto the test specimen and heated to approximately 1600°F and maintained near this temperature for about 100 hours.

Monitoring during the tests and post-test examinations provided information on temperature histories, gas release rate and composition, depth of sodium penetration into the concrete and sodium-concrete reaction product composition. Details of the LSC-2 and LFT-6 tests are reported in Reference A-8.

Several additional intermediate-scale tests (1 ft^2 concrete surface area) have been completed. Reference A-9 presents a comprehensive summary of all the sodium-concrete reaction tests completed as of December 1981, both in this development program and tests from other programs at U.S. labs and abroad. Reference A-16 is an executive summary of the sodium-concrete reaction test data and its application to limestone concrete.

A.1.3 Schedule

Additional tests scheduled in this development program are as follows:

<u>Tests</u>	<u>Description</u>	<u>Scheduled Completion</u>
1. Dolomite Aggregate Characterizations	This series of tests will determine differences, if any, in sodium reactions with calcitic limestone and dolomitic limestone aggregates.	July 1982
2. AB/AA Comparison Tests	This 4 test series will assess differences, if any, in results at HEDL and Sandia labs with both dolomitic and calcitic limestone concretes.	July 1982

<u>Tests</u>	<u>Description</u>	<u>Scheduled Completion</u>
3. LCT-Series	This 11 test series will investigate the effects on sodium-concrete reactions of CRBRP design features such as surface orientation (horizontal or vertical), presence of insulating concrete, restraint, external pressure, embedments in the concrete, and pre-dehydration (simulating delayed liner failures).	December 1982

4

A.1.4 Criteria of Success

In order to confirm the scenario for the Thermal Margin Beyond the Design Base evaluation, this program is required to evaluate the penetration and interaction of sodium with the reactor cavity concrete floor including the effects of a potential floor liner failure. The criteria of success are that the test program confirms that the sodium-concrete reactions are approximately as modeled and are self-terminating because of the buildup of reaction products, and that spalling and mechanical breakup of the concrete will not enable the reaction front to proceed through the concrete structure.

A.1.5 Fallback Position

In the event that the tests do not substantiate the current models that show that the sodium-concrete reactions are self terminating, the experimental results will be factored into the analyses along with other updated information and thermal margins will be provided.

A.2 HYDROGEN AUTO-CATALYTIC RECOMBINATION

A.2.1 Purpose

Hydrogen auto-catalytic recombination is important in assessing the Thermal Margin Beyond the Design Base as indicated in Section 3.2.2. The burning criteria are based on extensive experimentation (Reference A-4) including the following ignition tests:

- o Ignition of Hydrogen-Nitrogen Jets
- o Ignition of Hydrogen-Nitrogen-Sodium Jets
- o Ignition of Hydrogen-Nitrogen-Sodium-Water Jets
- o Effects of Oxygen Depletion on Hydrogen Burning
- o Hydrogen Formation in Sodium-Water-Air Atmospheres
- o Effects of Jet Velocity

and the following extinguishment tests:

- o Effects of Oxygen Depletion on Hydrogen Jet Burning Efficiency
- o Effects of Jet Sodium Concentration
- o Effects of Jet Velocity
- o Effects of Jet Temperature
- o Effects of Atmosphere Water Vapor Concentration

These tests were performed in a simulated containment vessel having a volume of 3.5 ft³. The remaining tests are aimed at confirming the validity of the burning criteria in a larger simulated test vessel. These tests employed a vessel having a volume of 3800 ft³, which provided a scaleup of a factor of more than 10³.

A.2.2 Program

To provide more prototypic conditions to assess hydrogen auto-catalytic recombination, three large scale tests involving sodium-concrete interactions were performed and hydrogen ignition characteristics were determined. A

simulated containment vessel having a volume of 3800 ft³ was attached to the sodium-concrete reaction test components. The oxygen concentration in the containment vessel can be controlled. The three tests run were:

- o LSC-2 (See Section A.1.2 for description)
- o LFT-6 (See Section A.1.2 for description)
- o LFT-5. This is similar to LFT-6 except that faulted liner conditions for FFTF were being simulated; below the faulted liner are firebrick, insulating brick, and refractory mortar above the basalt concrete test specimen.

For the naturally generated hydrogen from these tests, ignition conditions were determined in terms of the jet gas temperature, jet sodium concentration and the oxygen concentration of the simulated containment vessel.

A.2.3 Schedule

This development program has been completed and the final results are reported in Reference A-8.

A.2.4 Conclusions

The test results for the larger-scale tests were consistent with the small-scale results reported in Reference A-4, and gave further confirmation of the hydrogen burning criteria of Section 3.2.1 and Appendix C.1. No further testing is required.

A.3 FURTHER VALIDATION OF THE CACECO COMPUTER CODE

A.3.1 Purpose

The objectives of this activity were to further validate the CACECO computer code used in many of the analyses in this report. Initial validation is reported in References A-5 and A-6. In these references, the code and input data were validated using experimental results available through 1976 and some results from 1977. With the additional experimental data that subsequently became available, further confirmatory validation was performed under this development program.

A.3.2 Program

The further validation of the CACECO code included the following items:

1. A report has been issued, Reference A-10, which describes the analytical validation of the code. This included a comparison of the code with analytical solutions, other validated codes and hand calculations.
2. A revised users guide has been issued (Reference A-5) to provide updated user information.
3. A report has been issued (Reference A-11) which summarizes the experimental information used in the code and/or code input. The code and input data were compared with data from appropriate sodium-concrete and heated concrete tests, the HEDL hydrogen auto-ignition experiments, and appropriate concrete water release experiments.

A.3.3 Schedule

This development program has been completed and the final results reported in References A-10 and A-11.

A.3.4 Conclusions

The analytical and experimental validations of the CACECO code reported in References A-10 and A-11 provide confirmation that CACECO is a valid tool for assessing beyond design base thermal margins for the CRBRP. No further work is necessary under this development program.

A.4 COMPREHENSIVE TESTING PROGRAM FOR CONCRETE AT ELEVATED TEMPERATURES

A.4.1 Purpose

The purpose of this testing program was to establish a data base of the analysis and design of concrete exposed to elevated temperatures under conditions commensurate with nuclear power plant applications.

The specific objectives of this testing program were:

- a. To define the variations in the physical (thermal) properties of limestone aggregate concrete and lightweight insulating concrete exposed to elevated temperatures resulting from a postulated large sodium spill.
- b. To develop thermal relationships for use in the analysis and design of reinforced concrete components under high temperature conditions resulting from postulated large sodium spills in equipment cells.
- c. To define the variations in the mechanical (strength) properties of limestone aggregate concrete and lightweight insulating concrete exposed to elevated temperatures resulting from a postulated large sodium spill.
- d. To develop strength relationships for use in the analysis and design of reinforced concrete components under high temperature conditions resulting from postulated large sodium spills in equipment cells.

A.4.2 Program

The program of research specified in the Comprehensive Testing Program for Concrete at Elevated Temperatures defined the variations in the physical (thermal) and mechanical (strength) properties of prototypic CRBRP limestone aggregate concrete and lightweight insulating concrete exposed to elevated temperatures.

The Comprehensive Testing Program for Concrete at Elevated Temperatures consisted of two major phases. The scope of the testing program phases consisted of the following:

Phase I: Confirmation of Mechanical Properties

This phase consisted of testing to determine the effect of elevated temperature exposure on the strength properties of structural concrete and lightweight insulating concrete. A limited number of tests were performed on the lightweight concrete to determine its load response characteristics at penetration locations where localized crushing due to thermal expansion is likely to impact the penetration design. All testing were performed in an open moisture migration state while the concrete is at test temperature (open-hot condition). Each test sample was heated to test temperature at a rate of 30⁰F/hr and was heat soaked for 336 hours, unless otherwise noted, prior to mechanical testing. All samples were a minimum of 60 days old at the time of initial heat-up. The tests conducted are shown in Table A-1.

Part 1

Concrete cylinders 6" x 12" were tested for each temperature in the designated quantities in Table A-1 for the following parameters:

- a. Compressive Strength (f'_c)
- b. Modulus of Elasticity (E_c)
- c. Stress-Strain Relationship (σ versus ϵ)
- d. Moisture and Weight Loss
- e. Poissons Ratio (μ) (Standard Weight Concrete Only)

TABLE A-1

OPEN-HOT MOISTURE MIGRATION STATE

Test Temperature (°F)	Standard Weight Concrete (No. of Cylinders)	Lightweight Concrete (No. of Cylinders)
72°F (Control Cylinders)	3 (min) per each concrete batch	
150°F	6	3
225°F	6	3
350°F	6	3
500°F	3	3
700°F	3	3
900°F	3	3
1150°F	<u>3</u>	<u>0</u>
Total	30	18

* Three cylinders - (standard weight concrete only) for each of the above designated temperatures were heat soaked for approximately 672 hours prior to mechanical testing, to evaluate the long term heating effect on the mechanical properties of standard weight concrete.

Part 2

A sufficient number of tests (estimated below) were performed to determine with a high degree of accuracy the following properties for the temperature range 72°F to 1150°F for standard weight limestone aggregate concrete in the open-hot moisture migration system:

- a. The variation of concrete shear strength (v_c) with temperature (Approximately 24 specimens).
- b. The variation of concrete/rebar bond strength (u) with temperature (Approximately 24 specimens).
- c. The variation of sustained load (creep) characteristics with temperature (Approximately 15 specimens).

Phase II: Confirmation of Physical Properties

This phase consisted of testing to determine the effect of elevated temperature exposure on thermal properties of structural concrete and lightweight insulating concrete. The concrete properties investigated included: the instantaneous and average coefficients of thermal expansion, conductivity, specific heat, density, moisture migration rate and weight loss.

A sufficient number of tests (estimated below) were performed to determine with a high degree of accuracy the coefficients listed below over the temperature range of 72°F to 1150°F for standard weight and lightweight insulating concrete. The concrete was tested in an open moisture migration environment while at test temperature (open-hot condition). All samples were a minimum of 60 days old at the time of initial heat-up.

- a. Instantaneous and Average Coefficient of Thermal Expansion ($\bar{\alpha}_i$) and ($\bar{\alpha}$) of concrete at elevated temperatures.⁺
- b. Thermal Conductivity (k)⁺⁺
- c. Specific Heat (C_p)⁺⁺⁺
- d. Density at Elevated Temperatures (ρ)^{*}
- e. Moisture and Weight Loss^{**}

A.4.3 Schedule

Phase I of this program has been completed, and the final results are reported in Reference A-12. The Phase II tests have been completed and the final report is being prepared.

-
- + Approximately 3 specimens for each property
 - ++ 2 specimens for each material
 - +++ 6 specimens for each material
 - * Natural outfall of Phase I
 - ** Natural outfall of Phase I and Phase II, item d.

A.4.4 Conclusions

The mechanical properties of limestone concrete (Phase I tests) were determined and the results have been factored into the structural analyses. The Phase II tests have been completed and the results are being evaluated.

4

A.5 BASE MATERIALS TEST FOR LINER STEEL

A.5.1 Purpose

To obtain physical material data, under strictly controlled conditions, for the cell liner steel and weldment material.

A.5.2 Program

The experimental program was designed to produce tensile, creep and thermal expansion data on materials for the cell liners. The materials of interest are the cell liner steel, and the weldment material.

The base material and weldment materials underwent mechanical properties testing in the as-received condition. All tests were performed in an air atmosphere.

A.5.2.1 Uniaxial Tensile Tests

Uniaxial tensile tests were performed on the base material and the weldment materials to determine their temperature and strain rate dependency. All tests were performed in an air atmosphere. The number of tests for each material tested and the test condition are presented in the test matrix on the following page.

Number of Uniaxial Tension Tests
Per Material Type and Condition

Test Temp. (°F)	<u>Type 1 (Fig. A-1, A-2)</u> Base Material & Weldment (See Note 1)			<u>Type 2 (Fig. A-2)</u> Weldment (See Note 2)	<u>Type 3 (Fig. A-2)</u> Weldment (See Note 2)
	<u>A</u>	<u>B</u>	<u>C</u>		
Room Temp.	2	1	1	1	1
600	2	1	1	1	-
800	2	1	1	1	-
1000	2	2	2	1	-
1200	2	2	2	1	-
1400	2	2	2	1	-
1500	2	-	-	-	-
1600	2	2	2	-	-
1700	2	-	-	-	-
Totals: Weldment	18	11	11	6	1
Base Material	18	11	11	0	0

Note 1 - Column A at 10^{-4} in/in/sec strain rate

Column B at 5×10^{-3} in/in/sec strain rate

Column C at 10^{-1} in/in/sec strain rate

Note 2 - All type 2 and type 3 uniaxial tension tests were performed at the 10^{-4} in/in/sec strain rate. | 4

A.5.2.2 Creep and Stress-Rupture Tests in Air

Uniaxial creep tests in air were run over the temperature range 800°F to 1600°F, at 200°F intervals. Four stress levels were investigated at each | 4

temperature, in order to obtain meaningful creep and rupture relationships. The stress levels at each temperature were selected so that the rupture times would not exceed 500 hours.

A.5.2.3 Thermal Expansion Tests

In addition to the mechanical property tests described above, mean and instantaneous coefficients of thermal expansion were run to supplement existing data, limited to temperatures below 800°F. These supplementary tests were performed over the temperature range 700°F to 1700°F, at 100°F intervals. Two tests were run at each temperature for the ASME SA-516, Grade 55 material only.

4

A.5.3 Schedule

The tests originally planned for this development program have been completed. The test results for the base liner material were satisfactory, (Reference A-13) and have been factored into structural analyses. The test results for the weldment material did not satisfy ductility requirements for temperatures above 1000°F. An alternate weldment material possessing greater ductility has been proposed. Properties of the alternate weldment material and the need for additional testing are being assessed.

4

A.5.4 Criteria of Success

Since the purpose of the test is to establish materials properties, it is not possible to state a specific, quantitative success criterion. The tests will be successful when materials properties have been defined, with reasonable accuracy, over the range of interest. It is expected that the result will substantiate the data used in the present analysis.

A.5.5 Fallback Position

In the event that the test results do not confirm the adequacy of the data used in the present analysis, the results of this program will be factored in the analysis along with other updated TMBDB data.

A.6 SODIUM SPILL DESIGN QUALIFICATION TEST (LT-1)

This test program has been completed and information gained from the test has been factored into the scenario presented. Details of the test and the test results are presented in Reference A-14.

A.7 TMBDB AIR CLEANING SYSTEM PERFORMANCE TESTS

A.7.1 Purpose

Although the components which make up the TMBDB air cleaning system (quench spray chamber jet venturi scrubber and high efficiency fibrous bed scrubber) are commercially available and have been used in a variety of industrial applications, the performance of these components to the requirements of Section 2 in removing sodium and other reaction products generated during the CRBRP TMBDB scenario had to be demonstrated. This testing program confirmed the adequacy of the TMBDB air cleaning system.

The specific objectives of this program were:

- a. Confirm the performance of the TMBDB air cleaning system for conditions characteristic of the CRBRP TMBDB scenario.
- b. Provide data in support of the environmental qualification of the TMBDB air cleaning system equipment (quencher, venturi scrubber, high efficiency fiber bed scrubber and associated valves).

A.7.2 Program

A sodium aerosol was generated and aged in a test facility to simulate the in-containment conditions predicted from the CRBRP TMBDB scenario. These products were vented through the air cleaning system. The TMBDB in-containment conditions and air cleaning system flow rate were simulated. The parameters measured both upstream and downstream of each component are listed on the following page.

A state-of-the art report has been prepared to demonstrate the capability of the air cleaning system to remove fission products in the form of NaI, SeO_2 , and Sb_2O_3 (Reference A-7).

Data Requirements

The following in-containment data were obtained as a function of time during the conduct of the test:

- o atmosphere temperature
- o NaO concentration
- o NaOH concentration
- o Na_2CO_3 concentration
- o Metallic Sodium concentration
- o Particle electrical charge
- o containment absolute pressure
- o Na_2O concentration
- o particle size
- o total mass concentration
- o atmosphere concentration (% N_2 , O_2 , CO_2 , H_2)
- o relative humidity
- o determination of fallout % from appropriate data above

The following data were obtained outside of the containment atmosphere at these locations:

(a) Between the quench unit and venturi scrubber (b) between the venturi scrubber and high efficiency fibrous bed scrubber (c) between the high efficiency fibrous bed and the HEPA filter,* and (d) downstream of the HEPA filter.

- o temperature (both liquid & gas)
- o Na_2O concentration
- o NaOH concentration
- o flow rate ((a) and (c) only) (liquid and gas)
- o water solution concentration of NaOH, Na_2CO_3
- o particle size distribution

*The HEPA filter was a specific characteristic of the HEDL test, and is not part of the TMBDB design features.

- o Na_2CO_3 concentration
- o pressure differential across each component
- o removal efficiency of each component for particle size distribution

Additionally, the following specific information was obtained.

- o Quench unit humidity
- o Determination of % of sodium reaction products generated in the test facility which are vented through the air cleaning system.
- o Determination of % of duct and air cleaning equipment which becomes plugged by sodium reaction products.
- o Visual inspection of air cleaning system components at intervals of 24 hours of operation for any indication of degradation of performance or conditions which might be expected to preclude long term operation.
- o Evaluation of effect of increasing sodium reaction product (NaOH and Na_2CO_3) concentration in the water used for air cleaning equipment (separate water supplies should be provided for each unit (quencher, venturi scrubber, and high efficiency fibrous bed scrubber) in order that each component can be evaluated separately, and also so that an additional means for determining component removal efficiency can be provided).

A.7.3 Schedule

This development program has been completed and the final results are reported in Reference A-15.

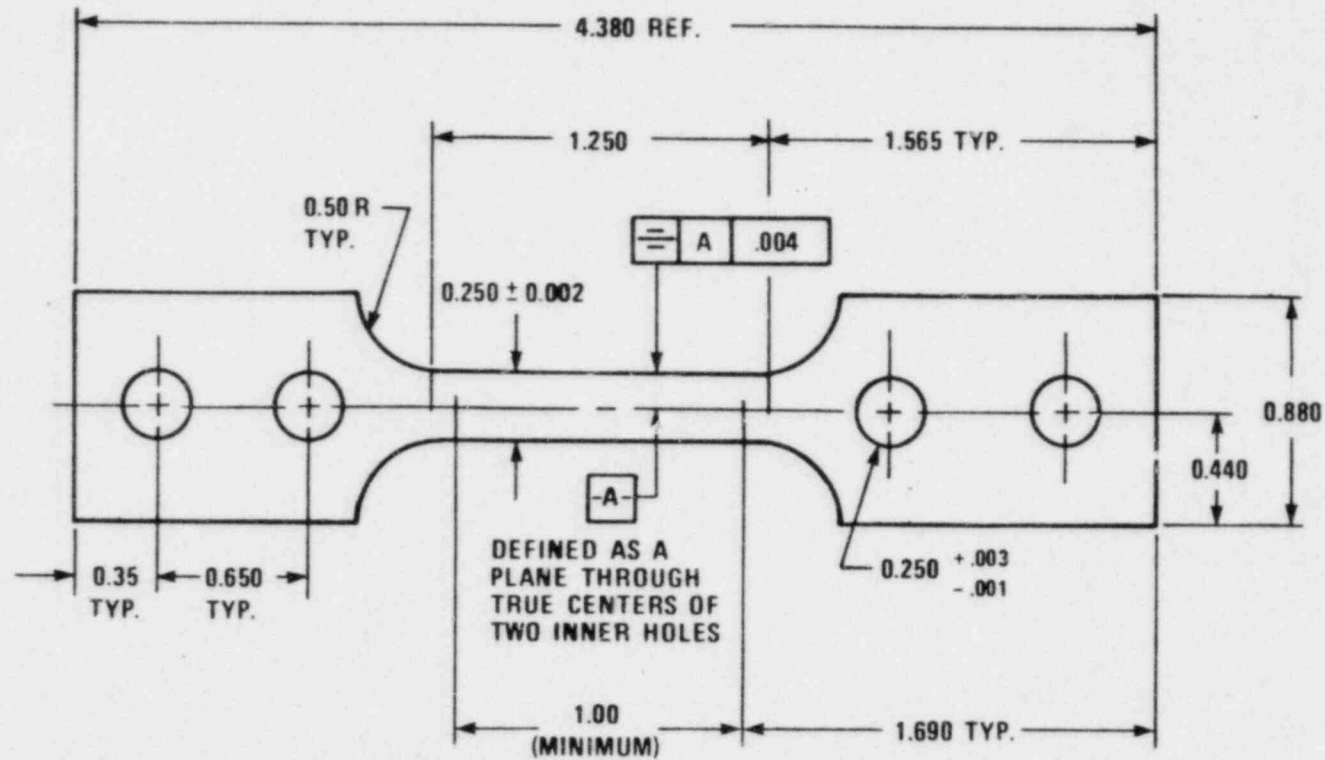
A.7.4 Conclusions

The test results showed satisfactory air cleaning system performance. The removal efficiencies exceeded those used in the radiological assessments (Chapter 4). No further testing is required.

A.8 REFERENCES

- A-1. J. A. Hassberger, "Intermediate Scale Sodium-Concrete Reaction Tests," HEDL-TME-77-99, August 1977. | 4
- A-2. R. K. Hilliard and W. D. Boehmer, "Concrete Protection from Sodium Spills by Intentionally Defected Liners, Small Scale Tests S9 and S10," HEDL-TME 75-75, July 1975.
- A-3 J. A. Hassberger, R. K. Hilliard and L. D. Muhlestein, "Sodium-Concrete Reaction Tests," HEDL-TME-74-36, June 1974.
- A-4. R. W. Wierman, "Experimental Study of Hydrogen Jet Ignition and Jet Extinguishment," HEDL-TME 78-80, April 1979.
- A-5. R. D. Peak, "Users Guide to CACECO Containment Analysis Code," HEDL-TME 79-22, June 1979.
- A-6 R. D. Peak, "CACECO Code Verification," in Fast Reactor Safety Technical Progress Report, April-June 1977, HEDL-TME-77-67.
- A-7 A. K. Postma and R. K. Hilliard, "Nucleation and Capture of Condensable Airborne Contaminants in an Aqueous Scrubbing System," HEDL-TME 78-82, September 1978.
- A-8 L. D. Muhlestein and M. W. McCormick, "Large-Scale Sodium-Limestone Concrete Reaction Tests LSC-2 and LFT-6," HEDL-TME 80-82, August 1981.
- A-9 A. K. Postma, L. D. Muhlestein and R. D. Colburn, "A Review of Sodium-Concrete Reactions," HEDL-TME 81-7, December 1981.
- A-10 R. D. Peak, "Analytical Validation of the CACECO Containment Analysis Code," HEDL-TME 79-2, August 1979. | 4

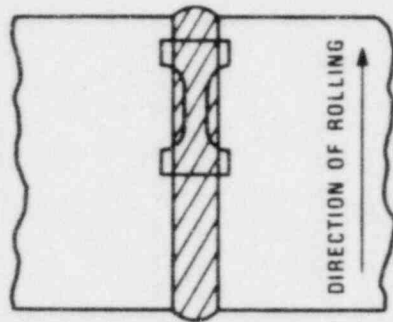
- A-11 R. D. Peak, "Experimental Validation of the CACECO Containment Analysis Code," HEDL-TME 80-13, April 1980.
- A-12 C. B. Oland, D. J. Naus and G. C. Robinson, "Final Report of Comprehensive Testing Program for Concrete at Elevated Temperatures," ORNL/BRP-80-5, October 1980.
- A-13 M. C. Cowgill, B. C. Gowda and K. C. Thomas, "CRBRP Final Report on Base Material Tests for Cell Liner Steels," CRBRP-ARD-0252, January 1980.
- A-14 L. D. Simmons and R. W. Wierman, "Large-Scale Liner Sodium Spill Test, LT-1," HEDL-TME 79-35, December 1980.
- A-15 R. K. Hilliard, J. D. McCormack, R. K. Owen, and A. K. Postma, "Aqueous Scrubber Air Cleaning System Demonstration for Containment Venting and Purging with Sodium Aerosols--CSTF Tests AC1-AC4," HEDL-TME 81-1, March 1981.
- A-16 L. D. Muhlestein and A. K. Postma, "Sodium-Concrete Reaction Executive Summary Report: Application to Limestone Concrete," HEDL-TME-82-15, June 1982.



ALL DIMENSIONS IN INCHES
 TENSION SPECIMEN THICKNESS = 0.250 INCHES
 CREEP-RUPTURE SPECIMEN THICKNESS = 0.150 INCHES

NOTE: SPECIMENS MEET THE DIMENSIONAL REQUIREMENTS
 OF ASTM E-8.

Figure A-1. Tension and Creep Rupture Test Specimens - Base Material

TYPE 1 SPECIMENSAPPROX. SIZE

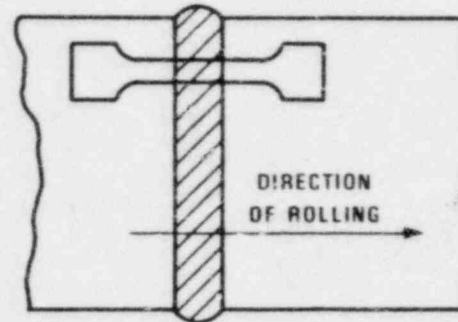
GAGE LENGTH	1"
WIDTH	1/4"
SPECIMEN LENGTH	4-3/8"
THICKNESS	1/4"
	(TENSION)
	15"
	(CREEP RUPTURE)

CONFIGURATION
ASTM E-8

NUMBER OF TESTS

TENSION	- 40
CREEP RUPTURE	- 20

DESIGN AS FOR PLATE MATERIAL

TYPE 2 SPECIMENSAPPROX. SIZE

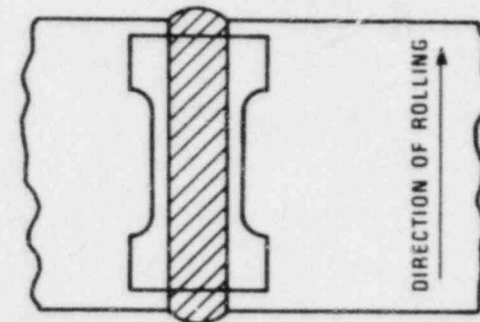
GAGE LENGTH	2"
WIDTH	1/2"
SPECIMEN LENGTH	8" MIN.
THICKNESS	~ 3/8"

CONFIGURATION ASTM E-8

NUMBER OF TESTS

TENSION - 6

SPECIMENS SHALL BE TESTED IN THE AS-WELDED CONDITION WITHOUT GRINDING OR FINISHING (IE: BACKING BAR SHALL BE LEFT IN PLACE).

TYPE 3 SPECIMENSAPPROX. SIZE

GAGE LENGTH	8"
WIDTH	1-1/2"
SPECIMEN LENGTH	18" MIN.
THICKNESS	~ 3/8"

CONFIGURATION ASTM E-8

NUMBER OF TESTS

TENSION - 1

GRIP ENDS SHALL BE OVERSIZED (l&w) TO ASSURE SUFFICIENT GRIP AREA DURING TESTING. THE GRIP END AREA ONLY SHALL BE GROUND SMOOTH. THE REMAINING AREA SHALL BE LEFT IN THE AS-WELDED CONDITION (IE: BACKING BAR SHALL BE LEFT IN PLACE).

Figure A-2. Tension and Creep Rupture Tests - Weldment Material

C.1.2 Heat Sources

C.1.2.1 Decay Heat

The decay heat is based on steady state operation at 975 MW without uncertainties - the nominal heat. The nominal decay heat is based on the homogeneous core design. The heterogeneous core design will have little or no impact on the scenario since the integrated decay heat over the first 24 hours is within 95% of the previous homogeneous design. Table C.1-3 gives the decay power for the various classes of fission products. The code uses a log-log interpolation technique to determine the power levels at intermediate times. | 4

The decay heat associated with the noble gases is input to the containment atmosphere at penetration of the reactor vessel and guard vessel. The heat associated with the halogens and volatiles is assumed to be contained in and carried with the sodium. The remainder of the decay heat is released at the bottom of the reactor cavity. This is a conservative approach, since some of the volatiles may boil away from the sodium pool before sodium boiling begins. Less decay heat in the reactor cavity would reduce the sodium boiloff rate and therefore would result in less severe containment conditions.

C.1.2.2 Sodium Activity

The energy associated with the decay of Na-24 was added to the sodium in both the reactor cavity sodium pool and the reactor cavity and containment atmospheres. The initial activity would be 25 milli-curies per cubic centimeter. The energy would decay with a 15 hour half-life.

C.1.2.3 Sodium-Concrete Interactions

The sodium-concrete reaction parameters used in this study are based on small and intermediate scale tests. These values are:

1. A penetration attack rate of 1/2 inch/hour (References C.1-2, C.1-3 and C.1-4).

2. A total penetration of 2 inches. The accumulation of reaction products limits the penetration depth. (Reference C.1-4).
3. A chemical heat release of 331 Btu/lb of concrete. (Reference C.1-2) This sodium-concrete reaction energy (Na-H₂O and Na-CO₂ reactions are considered in the next section) is only 5% of the decay power during the 4 hour reaction period, therefore, it is not a significant energy source and the conclusions of the analyses would not be impacted by considering the range of experimental uncertainty.

These reaction parameters are represented in the code as an energy input. The analysis assumed that the liner failure permitted sodium to attack the concrete across the full extent of the floor, or 1257 square feet, in the cavity.

C.1.2.4 Chemical Reactions

At the outset of the analysis, sodium vapor reacts with all of the oxygen in the cavity to form sodium oxide.

Sodium pool reactions occur next. When both water and carbon dioxide (from exposed heated concrete) are directed into the sodium pool, sodium reacts according to the molar ratio until either sodium or the carbon dioxide-water is consumed, producing sodium hydroxide or sodium oxide, sodium carbonate, carbon and hydrogen. The production of sodium hydroxide or sodium oxide is dependent on the hydrogen partial pressure and system temperature as presented in Figure C.1-2 (Reference C.1-18).

Upon reaching containment, the sodium vapor would react with the oxygen, carbon dioxide and water vapor according to their molar concentrations. The reaction with water vapor would take place if the water vapor concentration is greater than the oxygen concentration. If the water vapor concentration is less than the oxygen concentration the sodium vapor would react with oxygen and carbon dioxide according to their molar ratios.

Hydrogen reacting with oxygen is considered in the analysis, in the reactor containment building. The criteria for auto-ignition, are if either conditions (a) or (b) and condition (c) are met (see Appendix H.1).

C.1.5 References

- C.1-1 R. D. Peak, "Users Guide to CACECO Containment Analysis Code," HEDL-TME 79-22, June 1979.
- C.1-2 S. A. Meacham, "The Interaction of Tennessee Limestone Aggregate Concrete with Liquid Sodium," WARD-D-0141, December 1976.
- C.1-3 J. A. Hassberger, R. K. Hilliard and L. D. Muhlestein, "Sodium - Concrete Reaction Tests," HEDL-TME-74-36, June 1974.
- C.1-4 J. A. Hassberger, "Intermediate Scale Sodium-Concrete Reaction Tests," HEDL-TME-77-99, March 1978. (Availability: U.S. DOE Technical Information Center.)
- C.1-5 A. J. Ede, "Advances in Free Convection," in Advances in Heat Transfer, Vol. 4, pp. 1-64, Academic Press, New York, 1967.
- C.1-6 A. P. Colburn and O. A. Hougen, "Studies in Heat Transmission," Ind. Eng. Chem. 22, No. 5 pp. 522-539 (1930).
- C.1-7 J. G. Yevick and A. Amorosi, Fast Reactor Technology Plant Design, p. 413, MIT Press, Cambridge, MA, 1966.
- C.1-8 T. Z. Harmathy and L. W. Allen, "Thermal Properties of Selected Masonry Unit Concretes," J. Amer. Concrete Inst. 70, No. 2, pp. 132-142 (1973).
- C.1-9 E. Crispino, "Studies on the Technology of Concretes Under Thermal Conditions," Paper SP 34-25, Concrete for Nuclear Reactors, Vol. I, ACI SP-34, pp. 443-479, American Concrete Institute, Detroit, Michigan, 1972.
- C.1-10 T. Harada, J. Takeda, S. Yamane and F. Furumura, "Strength, Elasticity and Thermal Properties of Concrete Subjected to Elevated Temperatures," Paper SP 34-21, Concrete for Nuclear Reactors, Vol. I, ACI SP-34, pp. 377-406, American Concrete Institute, Detroit, Michigan, 1972.

- C.1-11 L. Baker, Jr., et al, "Postaccident Heat Removal Technology," ANL/RAS-77-2, Section VII, January 1977. | 4
- C.1-12 N. G. Zoldners, "Effect of High Temperatures on Concretes Incorporating Different Aggregates," Amer. Soc. Test. Mater., Proc. 60, pp. 1087-1108 (1960).
- C.1-13 A. K. Postma, J. D. McCormack and J. A. Schur, "A Study of Water and Gas Release from Heated Concrete," HEDL-TC-996, December 1977.
- C.1-14 J. D. McCormack and A. K. Postma, "Water and Gas Release from Heated Concrete," HEDL-SA-1117, 1976. | 4
- C.1-15 F. Kreith, Principles of Heat Transfer, Third Edition, Intex Educational Publishers, New York, 1973.
- C.1-16 G. H. Golden and J. V. Tokar, "Thermophysical Properties of Sodium," ANL-7323, August 1967.
- C.1-17 "Advanced Safety Analysis Fourth Quarterly Report June - August 1975," GEAP-14038-4, September 1975. | 4
- C.1-18 E. M. Mitkevich and B. A. Shikhov, "The Metallic Sodium-Sodium Hydroxide System," Russ J Inorg Chem, II, No. 3, pg. 343 (March 1966).
- C.1-19 L. D. Simmons and R. W. Wierman, "Large Scale Liner Sodium Spill Test, LT-1," HEDL-TME 79-35, December 1980. | 4
- C.1-20 D. G. Kroger and W. M. Rohsenow, "Condensation Heat Transfer in the Presence of a Non-condensable Gas," Int J Heat Mass Trans, II, pp. 15-26, 1968.

TABLE C.1-4
CHEMICAL REACTIONS

<u>Reaction Equation</u>	<u>Heat of Reaction</u>	<u>Type of Reaction</u>
* $2\text{Na} + \text{H}_2\text{O} = \text{Na}_2\text{O} + \text{H}_2$	1,600 Btu/lb Na	Pool
* $2\text{Na} + 2 \text{H}_2\text{O} = 2 \text{NaOH} + \text{H}_2$	4,514 Btu/lb Na	Pool
$4 \text{Na} + 3 \text{CO}_2 = 2 \text{Na}_2\text{CO}_3 + \text{C}$	4,326 Btu/lb Na	Pool
Na + Concrete	331 Btu/lb Concrete	Pool
$4 \text{Na} + \text{CO}_2 = 2 \text{Na}_2\text{O} + \text{C}$	3,800 Btu/lb Na	Atmosphere
$2 \text{Na} + \text{H}_2\text{O} = \text{Na}_2\text{O} + \text{H}_2$	3,400 Btu/lb Na	Atmosphere
$4 \text{Na} + \text{O}_2 = 2 \text{Na}_2\text{O}$	5,700 Btu/lb Na	Atmosphere
$2 \text{H}_2 + \text{O}_2 = 2 \text{H}_2\text{O}$	54,425 Btu/lb H_2	Atmosphere
$2 \text{Na} + \text{H}_2 = 2 \text{NaH}$	1,050 Btu/lb Na	Atmosphere
$\text{H}_2\text{O} + \text{Na}_2\text{O} = 2 \text{NaOH}$	1,500 Btu/lb Na	Atmosphere

*The production of sodium hydroxide or sodium oxide is dependent on the hydrogen partial pressure and system temperature as indicated in Figure C.1-2.

TABLE C.1-5
CONVECTIVE HEAT TRANSFER COEFFICIENTS

<u>Typical Values</u> (Btu/hr-ft ² -°F)	<u>Description</u>
1.21 at 700°F ΔT	Atmosphere of nitrogen (49%), hydrogen (49%) and sodium vapor (2%) inside the reactor cavity.
6.11 at 100°F ΔT	Atmosphere of hydrogen (21%) and sodium vapor (79%) inside the reactor cavity.
200.0	Natural convection film coefficients for sodium submerged surfaces.
1.13 at 75°F ΔT	Containment building and cell 105 atmospheres.
1.74 at 300°F ΔT	

- C.3-28 M. G. Cowgill, B. C. Gowda and K. C. Thomas, "CRBRP Final Report on Base Materials Tests for Cell Liner Steels," CRBRP-ARD-0252, January 1980.*
- C.3-29 H. Kupfer, H. Hilsdorf and H. Rusch, "Behavior of Concrete Under Biaxial Stresses," J. Amer. Concr. Inst. 66, No. 8, pp. 656-665 (1969).
- C.3-30 S. Freedman, "Properties of Materials for Reinforced Concrete," in M. Fintel, ed., Handbook of Concrete Engineering, pp. 141-211, Van Nostrand Reinhold Co., 1974.
- C.3-31 Letter from P. S. VanNort to R. S. Boyd, Transmittal of "Third Level Thermal Margins Report," Docket 50-537, S:L:977, April 22, 1976.
(Availability: Nuclear Regulatory Commission, Public Document Room.)

*The material concerning weldments in Reference C.3-28 became available after this Appendix was prepared and the structural evaluations described in Section 3.2 of this report were completed. The weldment properties will be taken into account in the final evaluation.

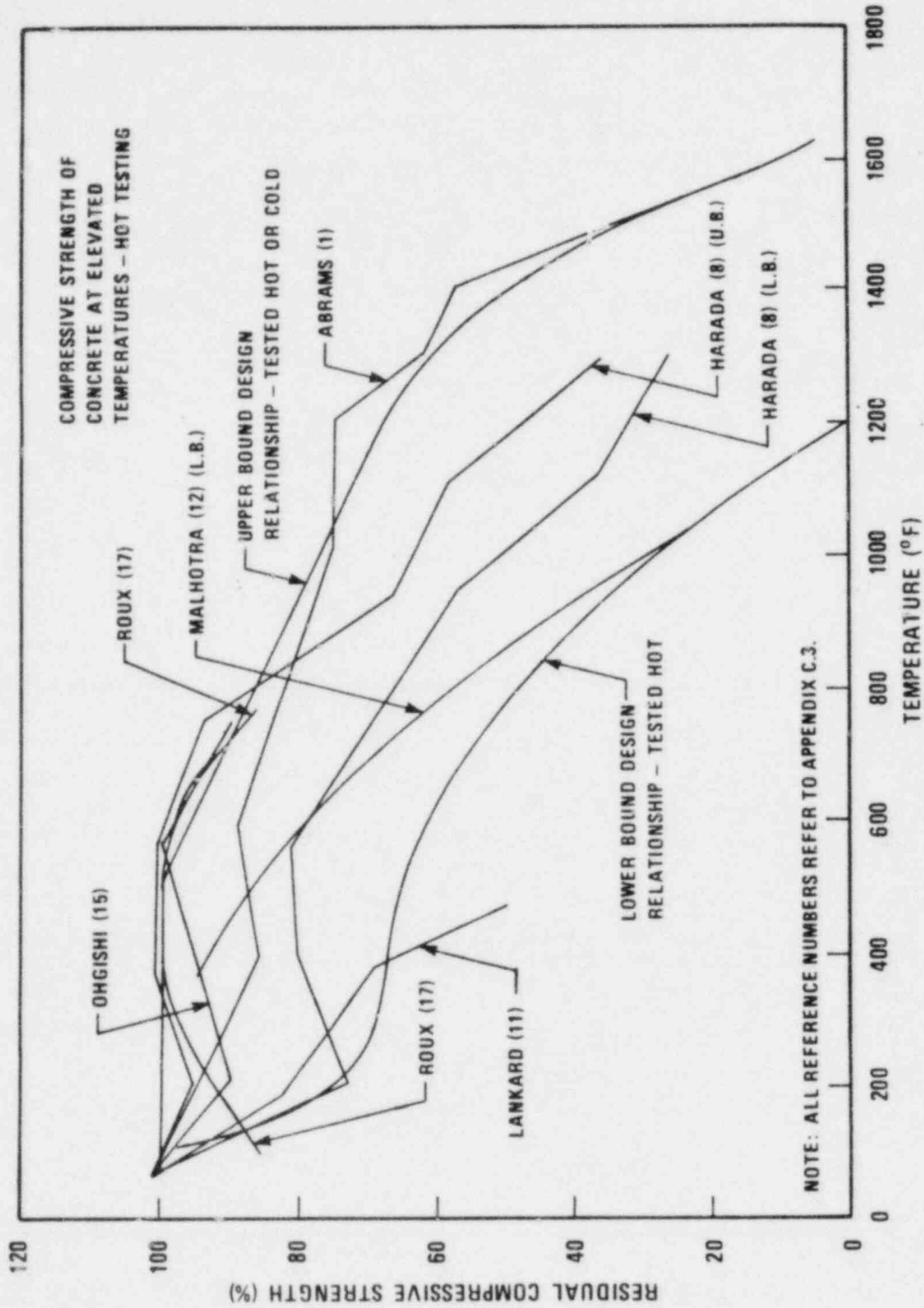


Figure C.3-1. Effect of Temperature Exposure on the Compressive Strength of Concrete - Hot Testing

G.2 CONSEQUENCES OF INCREASED SODIUM-CONCRETE REACTIONS

G.2.1 Introduction

Experiments (References G.2-1 through G.2-4) have indicated that sodium-concrete reactions are self-limiting for conditions occurring during the TMBDB scenario. These reactions have been represented in the reference case CACECO analysis as a penetration attack of 0.5 inch per hour for a period of 4 hours. This reaction rate is used in Section 3.2.2 as described in Appendix C.1. The sensitivity of the consequences to increased sodium-concrete interactions is examined here.

4

G.2.2 Model

The CACECO code model defined in Appendix C.1 was modified to perform these sensitivity studies. The model used in the reference case analysis in Section 3.2.2 includes a sodium-concrete reaction rate of 0.5 inch per hour for 4 hours, starting at the time of reactor cavity liner failure (assumed to be at the time of penetration of the reactor vessel and guard vessel). To assess the potential impact of more severe sodium-concrete reactions, the CACECO model was modified to consider reaction rates of 0.5 inch per hour for 12 hours and 1.0 inch per hour for 12 hours. The reaction energy was maintained constant at 331 Btu/lb of concrete. The sensitivity analyses were run for 30 hours without venting and the results were compared to the reference case.

G.2.3 Results

The two cases in which more severe sodium-concrete reactions were assumed are compared to the reference case described in Section 3.2.2. The additional energy from the more severe sodium-concrete reactions causes the sodium pool to heat up faster. Sodium boiling begins at about 9 hours in the reference case; this is reduced to about 8 hours with a sodium-concrete reaction rate of 0.5 inch/hr for 12 hours, and to about 7 hours with a sodium-concrete reaction

rate of 1.0 inch/hr for 12 hours. This additional energy source is reflected in slightly higher atmosphere temperatures in the reactor cavity and containment building and a higher containment steel temperature. However, as indicated in Figure G.2-1, these differences are minor and would not impact conclusions on the integrity of the containment.

Because of the additional energy source, the pressure in containment would be slightly higher (except for an early spike due to the treatment of hydrogen burning, discussed below). Again, the differences are minor as indicated in Figure G.2-2, and conclusions on containment integrity would not be impacted.

The hydrogen concentration in containment for the three cases is shown in Figure G.2-3. In all cases, the predicted hydrogen concentration at 24 hours and at 30 hours is zero. However, the short term (up to ~10 hours) concentrations vary slightly with the sodium-concrete reaction assumptions. With more severe reactions, the sodium pool heatup would be more rapid and the sodium vapor from the pool would be increased. This would result in the hydrogen burning criteria (described in Section 3.2.1) being met earlier (~8 or 9 hours compared to ~10 hours in the reference case). The maximum hydrogen concentration prior to the hydrogen burning would be decreased slightly (from 4.5% to ~4%). The analytic assumption of instantaneous burning when the criteria are met results in a predicted pressure spike as indicated in Figure G.2-2. The predicted spike is slightly less severe with increased sodium-concrete reactions but the variations are small enough to be of no consequence.

G.2.4 Conclusions

Table G.2-1 summarizes the results of these sensitivity studies on sodium-concrete reactions. The reference case considers a total depth of reaction of two inches of concrete. The sensitivity studies considered total depths of 6 inches and 12 inches. This provides factors of 3 and 6 on total energy from sodium-concrete reactions. The results show that the predicted

containment conditions are not very sensitive to the sodium-concrete reaction assumptions. This is due to the fact that the reaction energy from sodium-concrete reactions is a small part of the total energy involved in the scenario from decay heat, chemical reactions in containment and other chemical reactions in the sodium pool.

Since the containment conditions are similar for the range of sodium-concrete reactions considered, it is concluded that sufficient margin exists to cover the uncertainties in sodium-concrete reactions.

G.2.5 References

- G.2-1 J. A. Hassberger, R. K. Hilliard and L. D. Muhlestein, "Sodium Concrete Reaction Tests," HEDL-TME-74-36, June 1974.
- G.2-2 J. A. Hassberger, "Intermediate Scale Sodium-Concrete Reaction Tests," HEDL-TME-77-99, March 1978.
- G.2-3 L. D. Muhlestein and M. W. McCormick, "Large-Scale Sodium-Limestone Concrete Reaction Tests LSC-2 and LFT-6," HEDL-TME 80-82, August 1981.
- G.2-4 A. K. Postma, L. D. Muhlestein and R. P. Colburn, "A Review of Sodium-Concrete Reactions," HEDL-TME 81-7, December 1981.

TABLE G.2-1

SUMMARY OF SENSITIVITY STUDIES ON SODIUM-CONCRETE REACTIONS

Sodium-Concrete Reactions	Reference Case 0.5 in/hr for 4 hrs	0.5 in/hr for 12 hrs	1.0 in/hr for 12 hrs
<u>PRE-24 HOUR RCB CONDITIONS</u>			
Peak Hydrogen Concentration (%)	4.5	4.2	3.8
Time for Peak Concentration (hrs)	10.0	9.2	8.3
<u>24 HOURS RCB CONDITIONS</u>			
Atmosphere Temperature (°F)	450.0	480.0	520.0
Pressure (psig)	11.1	11.8	12.6
Steel Temperature (°F)	270.0	295.0	320.0
Hydrogen Concentration (%)	0.0	0.0	0.0
Oxygen Concentration (%)	13.7	13.3	12.7
<u>30 HOURS RCB CONDITIONS</u>			
Atmosphere Temperature (°F)	520.0	550.0	580.0
Pressure (psig)	12.5	12.7	13.4
Steel Temperature (°F)	315.0	335.0	360.0
Hydrogen Concentration (%)	0.0	0.0	0.0
Oxygen Concentration (%)	11.7	11.2	10.4

Results

Using the revised CACECO model, the containment conditions computed are listed in Tables G.4-1, 2 and 3 for the various cases. Tables G.4-2 and 3 indicate containment atmosphere temperature and pressure are more sensitive to the initial sodium release assumed than to the initial fuel release. The most severe results were found when 7,000 pounds of sodium and 7.5% of the fuel and solid fission products were assumed initially released to containment. The containment atmosphere temperature and pressure were found to be 1030°F and 24.4 psig. The containment metal temperature is not significantly affected by the sharp transient in atmosphere temperature because of its large heat capacity (at 1000 seconds the metal temperature is only 140°F). The containment could withstand all of the short term transients resulting from the initial head releases considered.

Conclusions

The calculations indicate that containment integrity after the initial release of fuel and fission products and sodium is not challenged for a wide range of assumptions. Considering the worst assumption (7,000 pounds of sodium and 7.5% fuel and fission products) containment integrity would be maintained following the initial head release. The general conclusion is that the TMBDB scenario has sufficient margin with respect to the amount of sodium and fuel assumed to be initially released.

TABLE G.4-1

EFFECT OF INITIAL FUEL, FISSION PRODUCT, AND SODIUM RELEASE*

		Dose (rem)		
		1% Fuel & F.P. 1000 lb. Na	5% Fuel & F.P. 3300 lb. Na	7.5% Fuel & F.P. 7000 lb. Na
	Bone	0.93	3.83	3.12
2 Hour	Lung	0.15	0.39	0.30
EB	Thyroid	11.3	9.51	5.19
	Whole Body	0.24	0.32	0.28
	Bone	55.7	56.2	55.8
30 Day	Lung	3.02	3.02	2.91
LPZ	Thyroid	5.31	1.72	0.83
	Whole Body	3.07	2.94	2.90

RCB Atmosphere Conditions**

Temperature (°F)	270	580	1030
Pressure (psig)	4.6	12.7	24.4

*Initial release of noble gases, halogens, and volatile fission products to RCB = 100%.

**Peak values for 1 hour.

TABLE G.4-2

EFFECT OF INITIAL FUEL AND FISSION PRODUCT RELEASE
WITH SODIUM RELEASE FIXED AT 1000 LB.

		Dose (rem)			
		<u>Initial Release of Fuel and Fission Products*</u>			
		<u>1%</u>	<u>5%</u>	<u>10%</u>	<u>50%</u>
	Bone	0.93	4.56	9.10	45.4
2 Hour	Lung	0.15	0.46	0.85	3.96
EB	Thyroid	11.3	11.3	11.3	11.3
	Whole Body	0.24	0.35	0.48	1.53
	Bone	55.7	58.5	60.6	83.7
30 Day	Lung	3.02	3.25	3.35	5.37
LPZ	Thyroid	5.31	4.43	3.53	3.53
	Whole Body	3.07	3.10	3.11	3.68

RCB Atmosphere Conditions**

Temperature (°F)	270	290	310	450
Pressure (psig)	4.6	5.0	5.7	9.5

*Initial release of noble gases, halogens, and volatile fission products to RCB = 100%.

**Peak values for 1 hour.

TABLE G.4-3

EFFECT OF SODIUM RELEASE FOR A GIVEN 10% FUEL-FISSION PRODUCT RELEASE*

		Dose (rem)	
		<u>Pounds of Sodium in Initial Release</u>	
		<u>0</u>	<u>1000</u>
	Bone	9.10	9.10
2 Hour	Lung	0.84	0.85
EB	Thyroid	11.2	11.3
	Whole Body	0.48	0.48
	Bone	63.5	60.6
30 Day	Lung	3.63	3.35
LPZ	Thyroid	5.28	3.53
	Whole Body	3.26	3.11

RCB Atmosphere Conditions**

Temperature (°F)	260	310
Pressure (psig)	4.6	5.7

*Initial release of noble gases, halogens, and volatile fission products to RCB = 100%.

**Peak value for 1 hour.

APPENDIX H
HYDROGEN BURNING CHARACTERISTICS

This Appendix provides the hydrogen burning characteristics used in the various analyses. Specifically, the hydrogen burning criteria are addressed in Appendix H.1, flame length considerations are addressed in Appendix H.2, and the potential for hydrogen stratification is addressed in Appendix H.3.

appropriate. It is noted that Regulatory Guide 1.7 applies the 4% limit to water reactor containments where the temperature, pressure, and water content are considerably above normal.

H.1.2.2 Detonation Limit for Hydrogen in Air

Reference H.1-1 gives the lower hydrogen concentration detonation limit in air at 18.3% at ambient conditions. Other experimenters (Reference H.1-4) observed the lower hydrogen concentration detonation limit to be as low as 14%. Shapiro and Moffette (Reference H.1-5), in their evaluation of the safety aspects for LWRs, use 19% as the lower hydrogen concentration limit for detonation.

The effect of TMBDB conditions on the lower hydrogen concentration detonation limit is not known; however, the magnitude of the effects would not be expected to be significant compared to the margin between the flammability and detonation limits. This is supported by the hydrogen burning experiments at HEDL that have indicated detonations occur under conditions similar to those in TMBDB only at hydrogen concentrations above 10%. The exact concentration was not determined from those experiments.

As Figure H.1-3 indicates, it would not be possible in the TMBDB scenario to reach a hydrogen concentration in which a detonation and resulting high pressures (7-15 atmospheres) would occur. This is because the large ignition source would cause the hydrogen to burn at the flammability limit (4% hydrogen) which is considerably below the detonation limit (14 to 19% hydrogen). It is noted that the large quantity of sodium entering containment would provide a continuous ignition source (satisfying criterion (b)), even if for some unknown reason the sodium would not burn, because sodium at 1700°F would be red hot.

Regulatory Guide 1.7 states that in water reactors with the oxygen content above 5%, the hydrogen concentration must not exceed 6% to insure that explosive concentrations are avoided.

H.1.2.3 Experiments Under Simulated TMBDB Conditions

Experiments have been performed at HEDL to study hydrogen burning under simulated TMBDB conditions (References H.1-6 and H.1-7). A conservative interpretation of the experiments indicated that hydrogen would burn when entering the containment if either criterion (a) or (b) is satisfied in combination with criterion (c).

- a. The hydrogen-nitrogen mixture entering containment is above 1450⁰F.
- b. The hydrogen-sodium-nitrogen mixture entering containment contains at least 6 g/m³ of sodium at temperatures above 500⁰F.
- c. The oxygen concentration is above 8%.

Criterion, (c) above, was found to be highly conservative. Figure H.1-4 reproduces the experimental results under the conditions that approach those of the TMBDB event. The two symbols indicate the oxygen content of the inlet and outlet gases in the simulated containment vessel. The average vessel oxygen content is between the inlet and outlet values - probably closer to the outlet value. As the figure indicates, hydrogen burning continues until oxygen levels decrease to ~4%.

H.1.3 Hydrogen Burning Scenario for TMBDB

The predicted hydrogen burning scenario will be presented in this section followed by a scenario that bounds the containment pressure and temperature conditions.

H.1.3.1 Predicted Hydrogen Burning Scenario

With respect to ignition of hydrogen entering the reactor containment building through the reactor cavity vent in the TMBDB scenario, the criteria used in the Section 3.2.2 analysis are appropriate and supported by the HEDL data (References H.1-6 and H.1-7).

4

With respect to hydrogen burning after ignition, when the oxygen content is reduced, applicable data are more numerous. Figure H.1-5 illustrates the burning limits from the HEDL experiments, the lower flammability limits derived by the U.S. Bureau of Mines and the flammability limit in Regulatory Guide 1.7. Considering that the HEDL data define when hydrogen burns as it passes through the sodium flame at the reactor cavity vent (establishing the 8% oxygen limit for complete hydrogen burning), and the Bureau of Mines data define the burning region in a hydrogen-air atmosphere with an ignition source (establishing the 5% oxygen limit for hydrogen burning above 4%), the predicted hydrogen burning scenario for TMBDB conditions is that shown on Figure H.1-6.

The complete hydrogen burning criteria are that hydrogen will burn when entering containment or within the containment when either criterion (a) or (b) is satisfied in combination with criterion (c).

- a. The hydrogen-nitrogen mixture entering containment is above 1450^oF.
- b. The hydrogen-nitrogen-sodium mixture entering containment contains at least 6 g/m³ of sodium at temperatures above 500^oF.
- c. The containment oxygen concentration is above 8%. With the oxygen concentration above 5% and the hydrogen concentration above 4%, the hydrogen in excess of 4% would burn.

H.1.3.2 Hydrogen Burning Scenario to Bound Containment Temperature and Pressure

Because of the possibility that hydrogen might burn at lower hydrogen concentrations than 4% in the presence of the large sodium ignition source, a bounding hydrogen burning scenario was developed to maximize the containment temperature and pressure effects. For this bounding case, it was assumed that all hydrogen burns if any oxygen is present in containment. This bound is indicated on Figure H.1-6.

H.1.4 Containment Conditions

H.1.4.1 Conditions Prior to Venting and Purging

Containment conditions were determined for the predicted and bounding hydrogen burning scenarios using the CACECO code model described in Section 3.2.2 and Appendix C.1. Figures H.1-7, 8 and 9 show the containment atmosphere temperatures, pressures, and hydrogen concentration for these cases as a function of time. Table H.1-1 provides the containment conditions at 24 hours for these cases. Figure H.1-10 indicates the containment conditions with respect to the flammability limits.

At 24 hours, the predicted scenario is identical to the bounding case that assumes complete hydrogen burning since the 8% oxygen cutoff value has not been reached. Consequently, no hydrogen accumulation is predicted in containment at 24 hours. Both cases indicate the containment does not require venting and purging until times beyond 24 hours.

Beyond 24 hours the pressure, temperature and hydrogen concentration of the predicted hydrogen burning case and the bounding case continue to climb. The pressure differential between the predicted burning case and the bounding case is an insignificant 1 psi. The atmosphere temperature differential is also small. The hydrogen concentration for both cases decreases between 45 and 48 hours. This is a temporary condition due to the formation of sodium hydride in the containment building. The reaction combines free hydrogen and sodium

H.1.6 References

- H.1-1 B. Lewis and G. von Elbe, Combustion, Flames and Explosions of Gases, Second Edition, Academic Press, Inc., New York, 1961.
- H.1-2 H. F. Coward and G. W. Jones, Limits of Flammability of Gases and Vapors, Bureau of Mines Bulletin 503, U.S. Bureau of Mines, Washington, D.C., 1952.
- H.1-3 G. W. Keilholtz, "Hydrogen Considerations in Light-Water Power Reactors," ORNL-NSIC-120, February 1976.
- H.1-4 W. E. Gordon, A. J. Mooradian and S. A. Harper, "Limit and Spin Effects in Hydrogen, Oxygen Detonations," Seventh Symposium (International) on Combustion, Oxford, Aug. 28 - Sept. 3, 1958, pp. 752-759, Academic Press, New York, NY. 1959.
- H.1-5 Z. M. Shapiro and T. R. Moffette, "Hydrogen Flammability Data and Application to PWR Loss-of-Coolant Accident," WAPD-SC-545, September 1957.
- H.1-6 R. W. Wierman, "Experimental Study of Hydrogen Jet Ignition and Jet Extinguishment," HEDL-TME 78-80, April 1979.
- H.1-7 L. D. Muhlestein and M. W. McCormick, "Large-Scale Sodium-Limestone Concrete Reaction Tests LSC-2 and LFT-6," HEDL-TME 80-82, August 1981.

TABLE H.1-1

CONTAINMENT ATMOSPHERE CONDITIONS AT 24 HOURS

	<u>Predicted Hydrogen Burning Scenario</u>	<u>Bounding Hydrogen Burning Scenario</u>
Atmosphere Temperature (°F)	450	450
Atmosphere Pressure (psig)	11.1	11.1
Hydrogen Concentration (%)	0.0	0.0

H.3 POTENTIAL FOR HYDROGEN STRATIFICATION

H.3.1 Introduction

During the TMBDB scenario, the potential for hydrogen collecting at the top of the containment dome in concentrations significantly greater than the average in containment (i.e., stratification) is different at different times in the scenario. There are three time frames in the base case scenario of interest, (1) early in the scenario, before hydrogen ignition (0 to 10 hours), (2) hydrogen burning period (10 hours to 133 hours), and (3) post-boildry period (133 hours to 8000 hours). In all three time periods there would be mixing forces in operation that are adequate to assure that no significant hydrogen stratification would occur.

In the initial period (1) the dominant mixing force would be forced convection turbulence due to the high velocity of the hydrogen jet entering containment through the reactor cavity vent. In the hydrogen burning period (2) the forced convection turbulence would still be in operation and mixing would be still further enhanced by the convection currents induced by the high temperature in the flame. In the post-boildry period mixing would be maintained primarily by the action of the vent/purge system.

It is noted that the hydrogen monitoring sample point is near the top of the containment dome, so that the higher concentration would be measured at all times.

H.3.2 Pre-Hydrogen Ignition Time Period

During the initial ten hours of the TMBDB scenario, hydrogen enters the reactor containment building at conditions which do not meet the burning criteria given in H.1.3.1. During this time period the hydrogen jet would have three forces acting to mix it with the RCB air; namely, molecular diffusion, natural convection and forced convection. As shown below, these

forces would be more than adequate to counteract buoyancy forces and prevent any significant collection (stratification) of hydrogen at the top of the RCB.

H.3.2.1 Molecular Diffusion

Molecular diffusion is a mass transfer process resulting from a concentration gradient existing between two locations. While the gradient exists, mass will flow from the region of high concentration to the low concentration region, and given sufficient time, this process can bring the system to an equilibrium state. For the TMBDB condition, however, the mass flow into the system, 84 lb/hr average, exceeds the diffusion mass transfer rate, 10-20 lb/hr, and this process would not, of itself, be adequate to prevent stratification even at the higher temperature existing after ignition at 10 hours. However, the diffusion process would supplement other processes.

H.3.2.2 Natural Convection

The hydrogen entering the reactor containment building from the reactor cavity is at a higher temperature than the containment shell. This difference in temperature could cause flow in the containment building which causes mixing. In the initial 10 hours of the scenario, the temperature differences between the incoming hydrogen and containment shell is less than a hundred degrees. Under these conditions, the buoyancy forces resulting from the temperature difference are not sufficient to overcome the buoyancy forces resulting from the concentration difference, and mixing of the streams due to natural convection flow would not be expected. After ignition at 10 hours, the temperature induced buoyancy forces are greater than the concentration induced buoyancy force, and free convective flow would occur, causing mixing of the fluid with the RCB.

H.3.2.3 Forced Convection

The major force that would mix the incoming hydrogen with the containment atmosphere is the turbulent action of the hydrogen jet. If the Reynold's number at the pipe exit exceeds 30, the flow quickly becomes turbulent downstream of the exit, and the turbulent action entrains fluid from the surrounding environment, Reference H.3-1 (see Figure H.3-1). The Reynold's number for the TMBDB scenario is 1400; thus, turbulent flow and significant entrainment would be expected.

Entrainment, a measure of the mixing, in a turbulent plume can be calculated by the formula $Q = .404 \sqrt{K} X$

where:

Q = volumetric flow rate of the plume at location X , ft^3/hr

$K = J/p, \frac{\text{ft}^4}{\text{hr}^2}$

$J = \text{momentum flux}, \frac{\text{lb-ft}}{\text{hr}^2\text{-ft}^2}$

$p = \text{density}, \text{lb}/\text{ft}^3$

$X = \text{distance from the jet exit}, \text{ft}$

It can be seen that as the distance from the jet exit increases, the quantity of material flowing in the plume increases; i.e., Q is a function of X . This occurs because of entrainment from the surrounding environment. Thus the difference between the quantity of material flowing at location X and the flow of hydrogen into the RCB is the amount of material from the RCB atmosphere which has been entrained.

Furthermore, the mean composition at location X is given by Q_0/Q_X where the subscripts 0 and X represent respectively, the origin and a specific location.

Table H.3-1 provides a calculation of the hydrogen concentration at a location 160 feet above the vent pipe outlet, the approximate intersection of the jet with the containment shell. From the table, it can be seen that, at this elevation, the hydrogen stream has been diluted to approximately 1.5% of its original concentration. Continued flow within the containment, induced by the injection of the hydrogen stream would cause further dilution, and in the limit, the concentration in the containment building would approach that of a well mixed tank.

H.3.3 Hydrogen Ignition to Sodium Boildry Time

After the hydrogen stream has been ignited, the surrounding air would continue to be entrained by the turbulent action of the jet (this is the means by which the flame gets its oxygen), and convection currents would be induced in the containment due to the large temperature differential between the combustion product gases and the containment building dome.

When venting and purging are initiated, the mixing action designed into the TMBDB vent/purge system would further enhance mixing even though this feature is not needed until the post-boildry period.

H.3.4 Post-Sodium Boildry Period

Long term (post boildry), the combustible gases expected to be produced by reactions within the reactor cavity are hydrogen and carbon monoxide which would be expected to form a mixture having a molecular weight similar to air because of the predominance of carbon monoxide (MW = 28) [see Section 3.2.3]. These gases would enter containment at high temperature and would probably not flow through the reactor cavity vent exclusively, due to the expectation that

many leakage paths would have opened by the time sodium has boiled dry (the base case scenario assumes leakage through the reactor head seals beginning at 50 hours). Furthermore, the flow rates are much lower late in the post-boildry period so that forced convection turbulence can no longer be counted on as the major mixing force. Thus, during this period the mixing action from the TMBDB vent/purge system would be the major force for preventing hydrogen stratification (and for breaking up any stratification that might occur late in the scenario if the vent/purge has been turned off for a time).

H.3.5 Conclusions

The potential for hydrogen stratification in the top of the containment dome has been assessed for the various conditions existing in containment throughout the TMBDB scenario. It is concluded that concentrations significantly higher than the containment average would not accumulate early in the scenario due to mixing forces inherent in the reactor cavity vent arrangement and the burning at the nozzle. Later in the scenario, stratification is prevented and/or dissipated by the mixing action of the containment vent/purge system.

H.3.6 References

- H.3-1. Schlichting, Hermann, Boundary Layer Theory, McGraw-Hill, 6th Edition, 1968, pp. 170-174, 696-702.

TABLE H.3-1
ATMOSPHERIC ENTRAINMENT IN HYDROGEN JET

Hydrogen Flow Rate	84 lb/hr
Pipe Diameter	1 foot
Pipe Velocity @ STP*	$\frac{84 \text{ lb}}{\text{hr}} \frac{1 \text{ lb-mole}}{2 \text{ lb}} \frac{359 \text{ ft}^3}{1 \text{ lb mole}} \frac{4}{\pi \text{ ft}^2} = \frac{19197 \text{ ft}}{\text{hr}}$
Fluid Density @ STP*	$\frac{2 \text{ lb}}{1 \text{ lb mole}} \frac{1 \text{ lb-mole}}{359 \text{ ft}^3} = 0.0055 \text{ lb/ft}^3$

$$K = \frac{\dot{m}v}{P} = \frac{(84)(19197)}{.0055} = 2.9 (10^8) \frac{\text{ft}^4}{\text{hr}^2}$$

$$Q @ 160' = (.404) (2.9)^{1/2} (10^4) (160) = 1,000,000 \frac{\text{ft}^3}{\text{hr}}$$

$$Q @ \text{origin} = \frac{84 \text{ lb}}{\text{hr}} \frac{\text{ft}^3}{.0055 \text{ lb}} = 15,000 \text{ ft}^3/\text{hr}$$

$$\% \text{H}_2 @ 160' = \frac{15,000}{1,000,000} = 1.5\%$$

Note 160' is the approximate vertical distance between the vent pipe outlet and the containment shell.

*The use of standard conditions gives a lower velocity and a higher density than those that would exist at higher temperatures. This in turn gives a lower (conservative) value of $\frac{J}{P} = \frac{mv}{P}$.

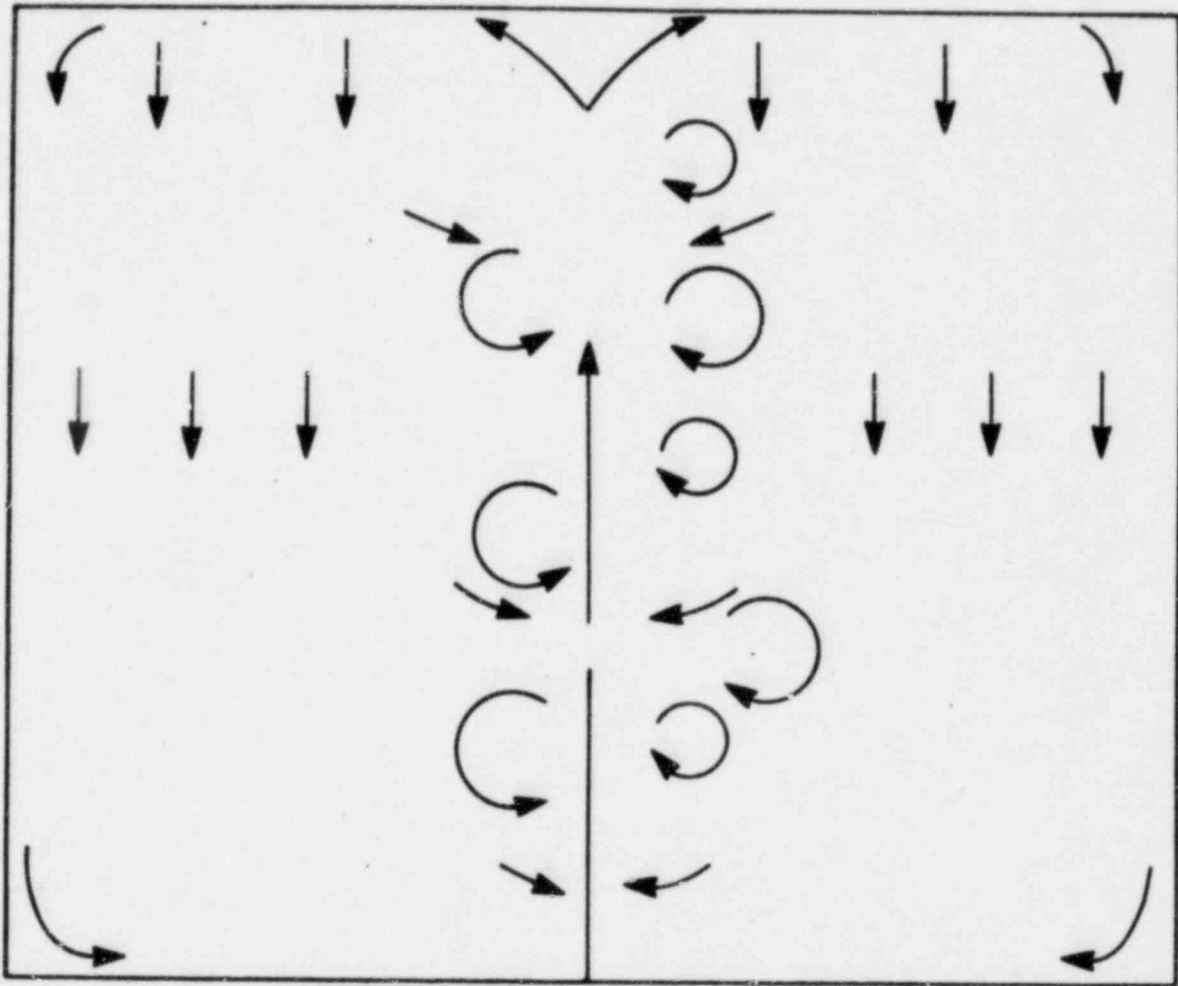


Figure H.3-1. Flow Patterns for Jet Injection Into a Closed Container

7184-2